5-2016

Differing Roles of the Great Plains Low-level Jet in Producing Warm Season Precipitation over the Central United States in 2002

Mengyuan Shang
University of Nebraska - Lincoln, mengyuan_s@hotmail.com

Differing Roles of the Great Plains Low-level Jet in Producing Warm Season Precipitation over the Central United States in 2002

by

Mengyuan Shang

A THESIS

Presented to the Faculty of

The Graduate College at the University of Nebraska

In Partial Fulfillment of Requirements

For the Degree of Master of Science

Major: Earth and Atmospheric Sciences

Under the Supervision of Professors Qi Hu and Robert Oglesby

Lincoln, Nebraska

May, 2016

Differing Roles of the Great Plains Low-level Jet in Producing Warm Season Precipitation over the Central United States in 2002

Mengyuan Shang, M.S.

University of Nebraska, 2016

Advisors: Qi Hu and Robert Oglesby

The purpose of this research is to describe and compare different roles of the Great Plains low-level jet (GPLLJ) in producing warm season precipitation over the central United States by model simulation. After going through 35 years' (from 1979-2013) NCEP North American Regional Reanalysis (NARR) data, year 2002 was selected for model simulation as it contained a "wet period" (May- June) and a "dry period" (July-August). The model simulation was done by using Weather Research and Forecasting (WRF) Regional Model. In this study, the GPLLJ was defined by the low-level wind at 925 hPa. The results showed the GPLLJ activities were stronger and more frequent in the "wet period" than in the "dry period". The 2-6 days' synoptic systems were also more active in the "wet period" than the "dry period". During the 2002 warm season, the wind direction of the GPLLJ was usually northward. Two cases, one from each period, were selected to compare the different roles of the GPLLJ in producing precipitation over central U.S. In the case chosen from the "wet period", there were two major effects of the GPLLJ on precipitation: 1) coupling with an upper-level jet streak (defined by the upper-level wind at 200 hPa) to create rising motion; 2) transportation of moisture into central U.S. The development of the GPLLJ and its effects on promoting precipitation were

largely associated with synoptic systems. However, in the case from the “dry period”, the effect of the GPLLJ was more emphasized on the transportation of warm, moist air from the Gulf of Mexico. With absence of synoptic system activities, the lift mechanism was provided by the weak warm front at the nose of the GPLLJ.

Acknowledgements

I would like to thank my thesis co-advisors, Dr. Qi Hu and Dr. Robert Oglesby for providing guidance and enlightenment for this study. I would also thank my committee member, Dr. Clinton Rowe for providing a wide variety of knowledge and experience to help accomplish this research. Finally, I would like to thank Michael Veres, for his guidance of setting up WRF for simulation and using the NCL for visualization model results as well as suggestions of this program. I would like to acknowledge the financial support of this study on this subject from the NOAA grant NA09OAR4310188 to the University of Nebraska-Lincoln. Computer resources for running WRF and NCL were provided by NCAR Yellowstone (http://n2t.net/ark:/85065/d7wd3xhc) and University of Nebraska-Lincoln's Holland Computing Center.

Contents

List of Figures

Chapter 3

Chapter 4

List of Tables

Chapter 3

Chapter 1

Introduction

Warm season precipitation is an important part of the annual cycle of precipitation over the central United States (U.S.). The central U.S. covers the area from Texas to North Dakota and Louisiana to Minnesota, about 30°-48°N, 105°-90°W. This warm season precipitation has pronounced effects on agriculture, industries and people's everyday lives. Better understanding and prediction of the warm season precipitation over the central U.S. therefore can affect decision making and prevent unnecessary property loss, especially during extreme precipitation events such as the 1993 flood and 1988 drought.

Warm season precipitation in the central U.S. area exhibits both seasonal and diurnal fluctuations. Maximum rainfall usually occurs in late-spring time (May and June) rather than summertime, and results from the strong convergence of water vapor flux associating with the baroclinic structure of continental scale circulation (Wang and Chen 2009). Heavy precipitation events frequently occurs around midnight, often related with convective activity (Higgins et al. 1997; Wallace 1975). Warm season precipitation area for the purpose of this work is defined as 35°-45°N, 90°-105°W, consistent with previous studies (Hu and Feng 2001; Pu and Dickinson 2014). Pu's work (2014) pointed out the nocturnal convective precipitation often occurs in the area 90°-100°W when afternoon maximum rainfall occurred more to the west, about 100°-105°W in the summertime, consistent with the development of rising motion and subsequent advection downstream. Eastward propagating convective systems from the Rockies to the Great Plains area are considered to be crucial for the nocturnal rainfall peak (Jiang et al. 2006) and two

categories of possible mechanisms are proposed: 1) density currents and various forms of trapped gravity waves in the planetary boundary layer (Carbone et al. 2002); 2) gravity–inertia waves in the free atmosphere (Carbone et al. 2002). The diurnal oscillation of the convective activities in summer is partly associated with the low-level convergence related to the passage of large synoptic disturbances (Wallace 1975). From North American Regional Reanalysis (NARR), it is suggested that the convergence of stationary moisture flux due to a coherent, anticyclonic circulation from the Gulf of Mexico contributes about three-fourths of the warm season precipitation in the central U.S. (Ruiz-Barradas and Nigam 2006).

The Great Plains low-level jet (GPLLJ) is a common phenomenon that occurs in the Great Plains region (Bonner 1968), and is considered to be an important influencing factor to warm season precipitation over the central U.S. Bonner (1968) defined 3 speed criteria for low-level jet (LLJ) events: the maximum wind speed must be equal or larger than 12 m/s, 16 m/s or 20 m/s. Revised criteria can be used to separate weak LLJ events ($12 \text{ m/s} \leq \text{Vmax} < 16 \text{ m/s}$), neutral LLJ events ($16 \text{ m/s} \leq \text{Vmax} < 20 \text{ m/s}$) and strong LLJ events ($\text{Vmax} \geq 20 \text{ m/s}$) (Arritt et al. 1997). For all criteria, the GPLLJ often has a duration of 1 hour or longer and stronger GPLLJ events tends to have longer durations (Mitchell et al. 1995; Wu and Raman 1998). The GPLLJ often shows as a southerly flow, with direction falls in the range of south to southwest (Arritt et al. 1997; Bonner 1968; Mitchell et al. 1995). Since strong southerly winds can transport moisture with or without a local low-level wind speed maximum, in some studies, a “southerly wind event” (SWE) is defined and used for analysis (Mitchell et al. 1995). When a low-level (below 3000m) southerly wind (between 120° and 240°) meet one or more of Bonner’s (1968) wind

speed criteria for low-level jet, it can be defined as a SWE (Arritt et al. 1997). The only difference between a LLJ event and SWE is SWE doesn't need to contain the local maximum wind speed, while the LLJ event must contain the local maximum wind speed. For this reason, SWEs contains two major categories: referred as "non-LLJ SWEs" and "southerly low-level jets" (SLLJs). It turns out that the non-LLJ SWEs have much less diurnal variability compared to the SLLJs (Mitchell et al. 1995). Non-LLJ SWEs occurred more often in the afternoon for the well-mixed boundary layer suppress the development of the local wind speed maximum (Mitchell et al. 1995).

The GPLLJ events can be separated into two seasons: the cold season from October to March and the warm season from April to September (Bonner 1968). In the following study, we are going to focus on the roles of warm season GPLLJ in producing rainfall over the Great Plains. According to Bonner's work (1968), the warm season GPLLJ often occurs in the area of 95°-100°W, which is extended to the area of 25°-35°N, 97°-102°W at about 900 hPa (Weaver and Nigam. 2008) and also to 25°-45°N, 90°-105°W (Pu and Dickinson. 2014) in the later work. In this study, we used 25°-35°N, 92.5°-102.5°W as the area of the GPLLJ. Based on observational wind data, the GPLLJ tends to intensify and occur more often in the warm season at about 800 meters above the ground (Bonner 1968). In August and September, the strength of the GPLLJ reaches its peak (Mitchell et al. 1995).

There are several hypotheses of the formation and development of the GPLLJ. One is that the formation of the GPLLJ is related to the eastern slopes of the Rockies (Holton 1967). Later work showed Rockies and the Sierras in Mexico are important to maintain the GPLLJ by providing physical blocking, thermal forcing and interactions

with the upper-level jet streaks (Ting and Wang 2006). Uccellini's work (1980) shows coupling with an upper-level jet streak can be beneficial to the development of the GPLLJ and leeside cyclogenesis and troughing can produce the pressure gradient needed for the development of the GPLLJ . Observational wind data suggested the GPLLJ is enhanced in the warm sector of an extratropical cyclone (Arritt et al. 1997; Mitchell et al. 1995). The formation of the GPLLJ is important, but not the main topic of this study. Instead, the focus of this study is on the roles of the GPLLJ in inducing or enhancing warm season precipitation.

One of the most important features of the strong GPLLJ is its strong diurnal cycle. A lot of work pointed out that the strong GPLLJ events have nocturnal peaks e.g. (Pu and Dickinson 2014; Weaver and Nigam 2008; Wu and Raman 1998); while weak GPLLJ events don't have much diurnal oscillations (Bonner 1968; Mitchell et al. 1995). Based on those work, the climatology of the GPLLJ dependents largely on the nocturnal phase of the GPLLJ (Helfand and Schubert 1995). Some of the explanations about the possible factors that promote the formation and development of the warm season GPLLJ mentioned above can also account for the nocturnal peak of the warm season GPLLJ (Holton 1967).

Because of the similar occurrence of nocturnal peak features of the GPLLJ and warm season precipitation, the GPLLJ has been considered as a significant cause of nocturnal peak of warm season thunderstorms in the Great Plains area (Bonner 1968; Higgins et al. 1997; Wallace 1975). Especially the strong GPLLJ events, they are usually associated with the extreme precipitation events. Such as in 1993 flood case, the strong GPLLJ seems play an important role in producing extreme rainfall (Arritt et al. 1997).

There are two main hypotheses about the contributions of the GPLLJ to the development and maintenance of convective systems. One is that the development of thunderstorms is related to the moisture convergence associated with the GPLLJ (Pitchford and London 1962). The GPLLJ is able to enhance convection by generating a dynamic instability as a result of its own development (Wu and Raman 1998). As mentioned before, the low-level rising motion is considered as a trigger for convective precipitation (McCorcle 1988; Wu et al. 1998) and its role in diurnal oscillations is caused by the diurnal variability of the GPLLJ. The mechanism was further studied by Pu (Pu and Dickinson 2014), showing that the decrease of the GPLLJ after midnight caused positive vorticity tendency change to the east of the GPLLJ core, led to atmospheric boundary-layer convergence and finally induced the development of rising motion.

The other hypothesis is that the GPLLJ transports warm, moist air from the Gulf of Mexico into the central U.S. area (Augustine and Howard 1991). In the subsequent analysis of data simulated by the Goddard Earth Observing System Atmospheric General Circulation Model (GEOS-1 AGCM), it is shown that about one third of the moisture that transported in to the Continental U.S. is by the LLJ, with most of the moisture is transported in the nighttime (Helfand and Schubert 1995).

According to these hypotheses, the convective precipitation should appear at the north or northeast region of the GPLLJ exit region (Bonner 1968; Chen et al. 1993). For that reason, studies about the GPLLJ's contributions to the warm season precipitation (especially the nocturnal peak) often use 35°-45°N, 90-100°W as the warm season precipitation area (Weaver and Nigam 2008).

However, judging by the simulated data by the General Circulation Model

(GCM), it is proposed that the GPLLJ may not be the reason of causing the nocturnal peak of the thunderstorms (Ghan et al. 1996). On the basis of a case study, it is implied the ability of the GPLLJ to transport moisture from the Gulf of Mexico into the Great Plains depends on the origin location of the GPLLJ (Wu and Raman 1998). For example, if the GPLLJ didn't originate from or pass over the region of the Gulf of Mexico, clearly it might have some problems transporting warm, moist air from the Gulf of Mexico. The nocturnal maximum of the thunderstorms may be a result forced by other processes. That might indicate that the role of the GPLLJ in producing warm season precipitation over the central U.S. is complicated.

Researches about warm season rainfall and influence factors are relying more and more on model simulation data because of limitations of spatial resolution and other factors of observational data. However, there is a critical issue about the analysis based on the model simulation data: how accurate the results of the models are? Obviously, the accuracy of the model simulation can be effected by many factors, such as the resolution of model and the combination of the parameterizations. Previous studies already showed models have problems simulating the nocturnal peak features of warm season precipitation and the GPLLJ: the three global atmospheric circulation models (AGCMs) didn't capture the observed nocturnal rainfall peak well enough (Cook et al. 2008; Lee et al. 2008; Lee et al. 2007). Even high-resolution Weather Research and Forecasting (WRF) Model failed to capture the extremely sharp, shallow nature of the GPLLJ (Tollerud et al. 2008). The simulation of eastward propagation of convection from the mountains to the Great Plains was also not simulated well (Lee et al. 2007). For proper validation, studies based on models (both global and regional) need to consider the

factors that may affect the accuracy of models, including resolution and parameterization.

The purpose of this study is to find and compare different mechanisms of how the GPLLJ interacts with other factors to promote precipitation over the study region. Synoptic scale systems are a major forcing we are interested in, as they can interact with the GPLLJ and create precipitation. We are interested to find out to what extent can the GPLLJ not just serve as a moisture source, but also help trigger the convection. To achieve this goal, the WRF regional climate model (Skamarock et al. 2005) was used to simulate the GPLLJ and precipitation from May to August of 2002. The model was set up with a high resolution and the model domain covered the U.S.

In chapter 2, the observational data used in this study will be described, as well as the methods. The preliminary work before running the model, settings of the model and model validation will be described in chapter 3. Chapter 4 will present the analysis of the model results, including the seasonal variability of the GPLLJ, precipitation, synoptic scale settings and moisture advection, as well as the case studies of the GPLLJ and precipitation over the Central U.S. Chapter 5 summarizes the results of seasonal variability of the GPLLJ, precipitation and the results from the case study evaluations, and describes the work that should be done in the future.

Chapter 2

Observational Data and Methods

2.1 Data

The purpose of this study is to find different roles of the GPLLJ in producing warm season precipitation over the central U.S. with different environment settings. To achieve this goal, several different datasets were used. These including 3 hourly and 6 hourly winds data (both zonal and meridional wind), total precipitation and other simulated atmospheric data for the warm season. Observed daily precipitation data was used for further model validation.

The winds, precipitation and other data used for preliminary analysis are from the National Centers for Environment Prediction (NCEP) North American Regional Reanalysis (NARR), provided by the National Oceanic and Atmospheric Administration (NOAA)/ Oceanic and Atmospheric Research (OAR)/Earth System Research Laboratory (EARL) Physical Sciences Division (PSD), Boulder, Colorado, USA [available for download from the Web site at http://www.esrl.noaa.gov/psd/]. The NARR (Mesinger et al. 2006) is a long-term (covers from 1979 to near present) climate reanalysis dataset for the North American Region. The spatial and time scale of the NARR data is sufficient to provide input data for running WRF regional model. The data we used in this study is NARR 3 hourly data with a spatial resolution of 32 kilometers (approximately 0.30°). The multiple level variables have 29 pressure levels, ranging from 1000 hPa to 100 hPa. In this study, we only need the warm season data, from May 1st to August 31st of the 35 years (from 1979 to 2013).

However, the NARR data is reanalysis data. We also need observed data to

validate the accuracy of the model results, especially the accuracy of precipitation data. We used NOAA Climate Prediction Center (CPC) U.S. Unified Precipitation data, provided by the NOAA/OAR/ESRL PSD, Boulder, Colorado, USA [available for download from the Web site at http://www.esrl.noaa.gov/psd/] to further validate precipitation simulated by WRF. The CPC accumulated daily precipitation data covers the Continental U.S. area and has been interpolated to a 0.25° ×0.25° resolution (Chen et al. 2008; Xie et al. 2010; Xie et al. 2007), even higher resolution than the NARR precipitation data. The CPC precipitation data using gauge analysis covers the time period from 1948 to 2006.

2.2 Methods

To determine the differing roles of the GPLLJ in producing warm season precipitation over the Great Plains area, this study can be divided into 3 main steps. In this study, the visualization of the data was done by using NCAR Command Language (NCL, version 6.3.0) [Software]. (2015). Boulder, Colorado: UCAR/NCAR/CISL/TDD. http://dx.doi.org/10.5065/D6WD3XH5)

The first step of this study is to determine which year to simulate. We attempt to find a year that has two periods: a relatively wet period and a relatively dry period. By comparing the activities of the GPLLJ, moisture advection and synoptic settings of those two periods, we are trying to gain a basic idea of the differences of climatology of large-scale forcing in those two time periods. As mentioned before, on the basis of previous studies, we used 25-35°N, 102.5-92.5°W as the area of the GPLLJ and 35-45°N, 105-90°W as the area of warm season rainfall. According to Bonner (1968), the low-level jet

usually occurs at about 800 meters above the ground. In this study, we used 925 hPa (about 700 meters above the ground) as the study level of the GPLLJ. For the purpose of finding a year that has two relatively long periods in warm season, we calculated the area averages of the winds and precipitation from May 1st to August 31st of the 35 years (from 1979 to 2013) in the interested area, then plotted the time series of the area averaged values. By comparing the 35 years' time series, a specific year was selected.

The second step is to run WRF ARW using the NARR data for the selected year. The model setup can heavily effect the accuracy of the model results. Previous studies pointed out one common problem of the model simulated data: the models tends to have difficulties simulate the nocturnal peak of the precipitation in the central U.S., which is one of the crucial features of the warm season precipitation (Cook et al. 2008; Lee et al. 2008; Lee et al. 2007). Because of the disadvantages of former model simulations, we expect WRF can capture the diurnal cycle of the GPLLJ better by using high spatial resolution and better combinations of parameterization. We ran WRF using a few combinations of parameterization and calculated the daily, nocturnal and daytime area averaged winds and precipitation of interested regions. Then time series of winds and precipitation of each parameter combination were plotted and compared to time series of NARR winds and precipitation calculated the same way. We also compared the time series of daily accumulated precipitation of model results with CPC rainfall data using the similar method. We compared 6 hourly model results of winds, precipitation and sea-level pressure with corresponding NARR data. After the comparison, we chose and used the parameter combination that simulated the diurnal cycles of the GPLLJ and precipitation the best. According to previous study (Lee et al. 2010), the cumulus

parameter option is one of the most important factors that can affect the accuracy of WRF simulation, which is a key aspect of parameterization testing. We focused on testing two cumulus parameters: the Grell-Freitas (Grell and Freitas 2013) scheme and the Kain-Fritsch(Kain 2004) scheme according to Liang's work (Liang et al. 2004). It turned out for the selected year, judging by the time series, the Grell-Freitas scheme simulated the nocturnal peak of rainfall better than the Kain-Fritsch scheme.

By going through the 6 hourly model output data, we found two precipitation cases coincident with a strong GPLLJ. By comparing and contrasting the GPLLJ and large-scale synoptic background settings of those two cases, we would expect to identify the differing roles of the GPLLJ in producing warm season precipitation and the potential mechanism of this process as well.

Chapter 3

Model Experiments and Validation

3.1 Year Selection

Numerous papers have pointed out that a major disadvantage of using model simulated data to study this topic is the failure of properly simulating the nocturnal peak feature of the precipitation over that area (Lee et al. 2008; Lee et al. 2007). They also mentioned this inaccuracy of model maybe caused by course resolution or the combination of physical parameters settings. In order to better capture the important nocturnal peak feature of the rainfall, we used high spatial resolution and tested various combinations of physical parameters. Because of the extensive computing resources and time limitations, we selected one year to do the simulation then analyze the model results.

For this further analysis, we therefore attempted to find one year that contains two time periods in the warm season: a relatively wet time period and a relatively dry time period. By comparing the differences between the GPLLJ activities and the synoptic scale backgrounds through those two time periods, we can find different mechanisms of how the GPLLJ can promote precipitation by interacting with different scale systems.

As mentioned in the section 2.2, on the basis of previous studies, we used 25-35°N, 102.5-92.5°W as the area of the GPLLJ and 35-45°N, 105-90°W as the area of summertime rainfall over the Central U.S. Based on existed studies (Weaver and Nigam 2008), we used 925 hPa winds as the criteria of the GPLLJ in the following analyses. We calculated the averages of meridional wind, zonal wind and rainfall of interested areas using NARR data and plotted time series from May to August of 35 years, from 1979 to 2013. By going through 35 years' winds and precipitation data (figures not shown), year

2002 was selected as the target year to do the model simulation. In the central U.S., there is usually more precipitation in May and June than in July and August. (Wang and Chen 2009). From the time series, we can see in 2002, this general precipitation pattern was shown particularly well compared to other years. There were many more strong precipitation events in late-spring (May and June, referred as the "wet period") than in summertime (July and August, referred as the "dry period"). The diurnal cycles of the winds and precipitation were also different in those two time periods, indicating different mechanisms of how the GPLLJ influenced precipitation.

On account of the importance of the diurnal cycles of both the GPLLJ and precipitation, we plotted the time series of daily, nocturnal and daytime averaged winds and precipitation of interested areas. The time series of area averaged winds and precipitation for the 2002 warm season are showed in Figure 3.1. The daily averaged data were calculated from 03Z to 00Z of the next day since NARR data we used is 3 hourly. For the nocturnal time period, we calculated the averages of winds and rainfall from 03Z to12Z (9 p.m. Central Standard Time (CST) of the day before to 6 a.m. CST), while daytime time period was calculated from 15Z to 00Z of the next day (9 a.m. CST to 6 p.m. CST). The seasonal averages of daily, nocturnal and daytime area averaged winds and precipitation are shown in Table 3.1. From the results showed in Table 3.1, we can see the magnitude of meridional wind was much larger than zonal wind for all daily, nocturnal and daytime values. The daytime seasonal averages wind speeds were both smaller than the nocturnal hours. The seasonal averaged zonal wind direction was easterly for all daily, nocturnal and daytime time periods when meridional wind direction was southerly.

	Zonal wind (m/s)	Meridional wind (m/s)	Precipitation (mm/12hours)
Daily	-2.09	4.89	2.79*
Nocturnal	-2.27	6.17	1.71
Daytime	-1.90	3.61	1.07

Table 3.1 Seasonal averages of area averaged NARR daily, nocturnal and daytime meridional wind, zonal wind and precipitation from May 1st to August 31st, 2002. The unit of daily precipitation (denote by "*") is mm/24hours.

The standard deviations of daily, nocturnal and daytime area averaged winds and precipitation are showed in Table 3.2. The standard deviations of the meridional winds were about twice as large as the zonal winds for daily, nocturnal and daytime time periods. This implies that for the warm season, the directions and magnitudes of meridional winds changed more frequently than zonal winds.

	Zonal wind	Meridional wind	Precipitation
Daily	1.70	3.51	2.62
Nocturnal	1.93	3.89	1.89
Daytime	1.61	3.40	1.20

Table 3.2 Standard deviations of area averaged NARR daily, nocturnal and daytime meridional wind, zonal wind and precipitation from May 1st to August 31st, 2002.

Overall, for the warm season GPLLJ, meridional wind was more influential than zonal wind. Also, it is clear that from the seasonal averages that both the zonal and meridional wind speeds of nocturnal hours were larger than the daytime hours, especially the nocturnal meridional wind speed. That conclusion is consistent with former studies showing that the GPLLJ has a nocturnal peak (Pu and Dickinson 2014; Weaver and Nigam 2008; Wu and Raman 1998).

The average of nocturnal precipitation was also greater than the daytime precipitation, consistent with results of previous studies (Higgins et al. 1997; Wallace 1975) according to Table 3.1. Also, there were more intense precipitation events during

the nocturnal time period, such as the precipitation event around May 24th judging by Figure 3.1. Combined with previous research conclusions (Wallace 1975), the rainfall events that occurred in the nocturnal hours were likely caused by convective systems. Since the time series were plotted with winds and precipitation data averaged over interested areas, it is normal that the magnitudes of winds and precipitation were smaller. In this case, we can only use the time series as a basic view of the occurrence of the GPLLJ and precipitation events of the warm season in 2002, especially those strong cases. It is inappropriate to use them as the criteria to select individual GPLLJ case for further analyses. The seasonal change of the GPLLJ is also shown in Figure 3.1. In all daily, nocturnal and daytime time periods, more southerly meridional wind events with greater magnitude occurred in May and June. In July, the number of strong southerly wind decreased compared to former two months. In August, the southerly wind became strong again, but not as strong as in May and June. Also, the change of wind between days was strongest in May and June. That may imply the importance of synoptic forcing.

To sum up, in 2002, May and June had more precipitation events and July seems to be a relatively dry time period. In August, the amount of rainfall increased again. In addition to that, the nocturnal precipitation amount and frequency were greater than the daytime precipitation amount and frequency in May and June. On the contrary, in July, stronger precipitation tended to happen in the daytime (e.g. the precipitation case around July 10th). Figure 3.1 shows the diurnal cycle of rainfall as well. We can see the amount of precipitation was larger in the nocturnal hours than in the daytime period. However, because of the time series show the area averaged information, the nocturnal peak feature of precipitation might be weakened.

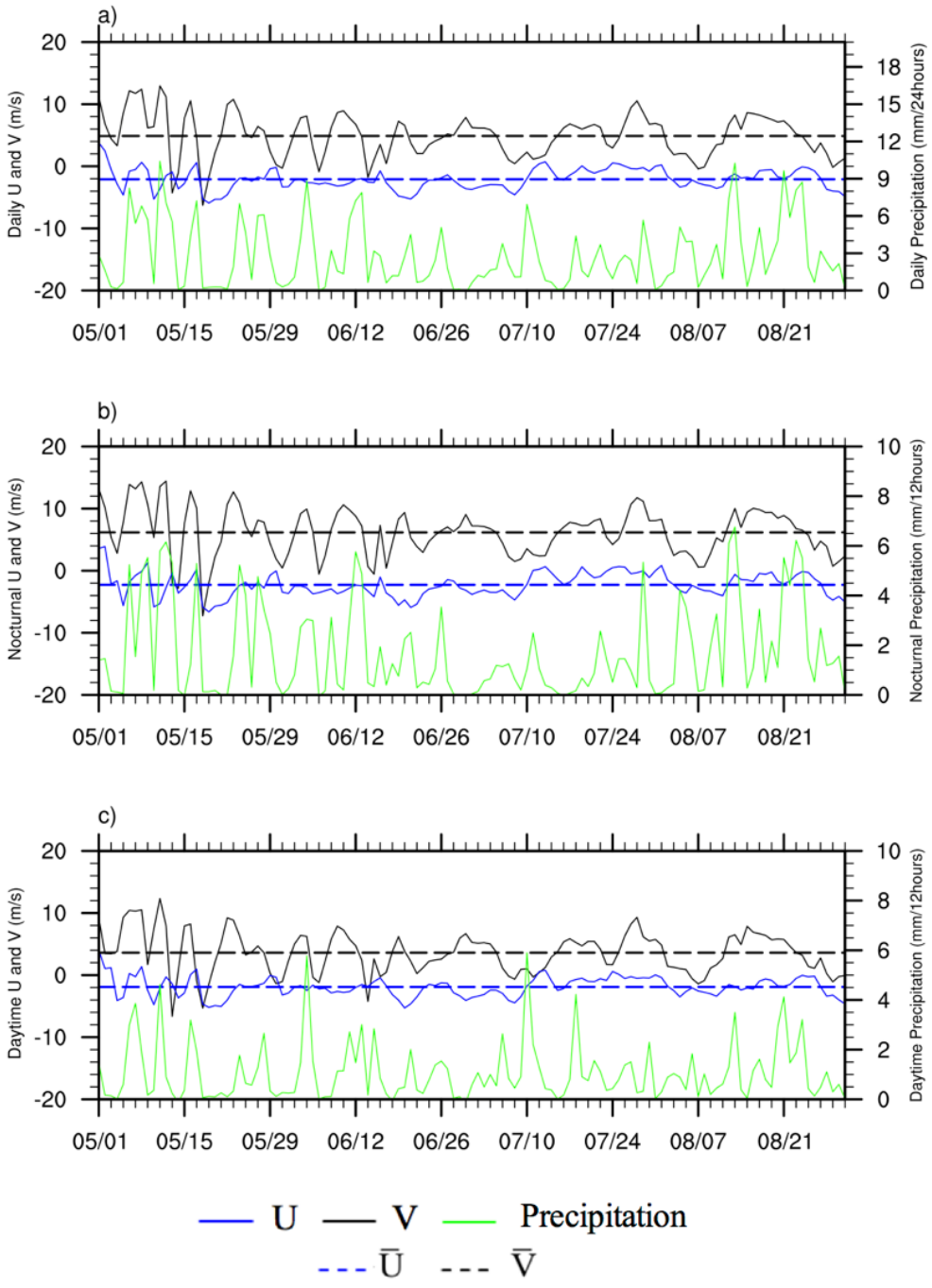

Figure 3.1 Time series of area averaged NARR 925 hPa U (zonal wind), V (meridional wind; 25-35°N, 102.5-92.5°W; units: m/s) and precipitation (35-45°N, 105-90°W; units: mm/24hours for a) and mm/12hours for b) and c)) of daily, nocturnal and daytime averages from May 1st to August 31st 2002. $\bar{U}$ and $\bar{V}$ are seasonal averages of U and V respectively. a), b) and c) shows daily, nocturnal and daytime U, V and precipitation respectively.

Uniting all these characteristics, we believe the year 2002 is a good year for simulation and further analysis. In the following chapter, we focused on analysis the cases chosen from the warm season of 2002.

3.2 Model Settings

In this study, we used regional model WRF-ARW, version 3.5. The domain used in the simulation covers the whole continental U.S. and the Gulf of Mexico, shown in Figure 3.2. Since numerous studies have shown the GPLLJ contributes to warm season rainfall by transporting moisture from the Gulf of Mexico into the Great Plains area (20°-50°N, 120°-75°W; Helfand and Schubert 1995), it is necessary to include the Gulf of Mexico in the domain. The GPLLJ and precipitation areas used to calculate the area averages of the winds and rainfall are also shown in Figure 3.2. As mentioned in chapter 1, the precipitation area is usually at the north nose region of the GPLLJ. As local air is shoved out of the way of the GPLLJ area and lifted due to the moisture transportation theory in former studies (Augustine and Howard 1991; Helfand and Schubert 1995).

In the model simulation, we used 3 hourly NARR data from April 15th to August 31st, 2002 to provide the large-scale forcing. For the consideration of the accuracy of model results, we started the simulation two weeks before May 1st. Because of the spatial resolution of NARR data is 32 kilometers and WRF performs better when the spatial resolution's ratio of outer and inner domain is 3:1, we set 10 kilometers as the resolution of WRF simulation for year 2002, which is very high resolution compared to previous model simulations of topics related to warm season precipitation in the central U.S. We are expecting that the higher resolution used here can lead to more accurate simulation

results, especially for precipitation simulation.

Testing of the cumulus parameterization options was one of the most important parts of model set up. We tested several cumulus parameters, including the Grell-Freitas (Grell and Freitas 2013) scheme and the Kain-Fritsch (Kain 2004) scheme. We compared the model results of winds and precipitation using different schemes with NARR data by plotting the time series of daily, nocturnal and daytime area averaged winds and rainfall. The nocturnal maximum of precipitation was simulated a little better using the Grell-Freitas scheme than using the Kain-Fritsch scheme. Liang et al. (2004) indicated that the Grell-Freitas scheme in the cumulus parameterization can capture the maximum nocturnal precipitation in the central U.S., and eastward propagation of convective systems as well. Judging by all above, Grell-Freitas was used as the cumulus parameter in the WRF simulation.

The testing of parameterization combinations in this study only shows the better physics options for 2002's model simulation. More tests of physics options can be done for different year and different input data to get more accurate model outputs.

For the consideration of how higher resolution model results can simulate convective systems better, two spatial resolutions were also tested with Grell-Freitas scheme as the cumulus option. In the preliminary tests of model set up, we tried 12 kilometers as the middle domain's resolution and 4 kilometers as the inner domain's resolution. The middle domain covers the continental U.S. and the Gulf of Mexico and the inner domain covers the central U.S. area. Another resolution tested was 10 kilometers with domain size shown in Figure 3.2. We compared the 10 kilometers and 4 kilometers resolutions' precipitation results. It turned out that there were no obvious

advantages to the 4 kilometers resolution. In consideration of computing resources and

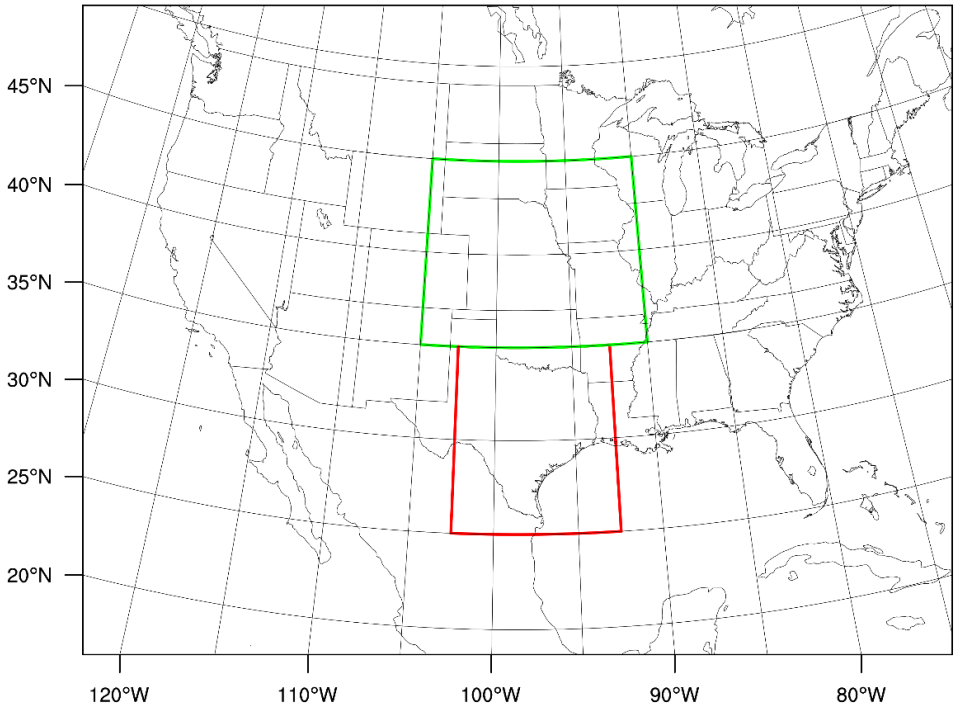

Figure 3.2 Domain of the model simulation and interested areas of the GPLLJ and precipitation. Red box is the GPLLJ area (25-35°N, 102.5-92.5°W). Green box is the precipitation area (35-45°N, 105-90°W).

time the model takes to run, 10 kilometers therefore seemed to be a better choice for this study.

Model validation is an important step after getting the model results. It is essential to make sure the model can capture the basic and important features of the variables. The next section therefore focuses on model validation.

3.3 Model Validation

The validation of model results can be done from two aspects: 1) plotting the time series of averaged winds and rainfall of interested areas and comparing the model results with NARR data; 2) validating model daily precipitation with NARR and CPC daily

rainfall data. Since this study mainly focused on the effects of the GPLLJ on warm season precipitation, the accuracy of winds and precipitation is of great importance. By plotting the daily, nocturnal and daytime averaged winds and rainfall, we anticipate the model can capture the diurnal cycle and seasonal variability of the GPLLJ and precipitation in the central U.S. However, the time series only show the area averaged information, but not the spatial patterns. The patterns of precipitation are especially vital for this study. Since NARR data is also a model product, it is possible that NARR's precipitation may not be close to actual observations. In view of this problem, high resolution observed precipitation data is also needed to support the results from WRF. For that reason, CPC rainfall data was used for further validation.

Figure 3.3 shown the area averaged winds and rainfall information from May 1st to August 31st, 2002 from model simulation. The calculations of area averages of winds and precipitation were similar to the calculations of plotting NARR data in Figure 3.1. However, since WRF data is 6 hourly data in this simulation, we calculated the daily averaged winds and accumulated precipitation from 06Z to 00Z of the next day (12 a.m. CST to 6 p.m. CST). The nocturnal period was calculated from 06Z to 12Z (12 a.m. CST to 6 a.m. CST) and the daytime period were calculated from 18Z to 00Z of the next day (12 p.m. CST to 6 p.m. CST). The other difference is because the resolution of WRF is higher than the resolution of NARR, we interpolated WRF data to 0.125° × 0.125° field when NARR data was interpolated to 0.25° × 0.25° field, close to each resolution. In this way, we are trying to avoid unnecessary deviations caused by calculation. The seasonal averages of daily, nocturnal and daytime area averaged winds and precipitation are showed in Table 3.3 and the standard deviations of the same variables are shown in Table

3.4. The seasonal averages of winds and precipitation of WRF simulation have smaller values compared to NARR data. Comparing with NARR data, seasonal averages of winds and precipitation of WRF simulation were all smaller in daily, nocturnal and daytime averages, though the relationships were similar. The directions of seasonal averaged winds were the same in WRF and NARR data: zonal winds were generally easterly and meridional winds were southerly. Judging by the seasonal averaged daily, nocturnal and daytime values, the magnitudes of meridional wind were all greater than zonal wind. From Table 3.4, we can see the patterns of standard deviations of WRF winds and precipitation are also similar to NARR data. The magnitude and direction of meridional wind changed more frequently compared to zonal wind. That indicates the meridional wind was more important in defining the GPLLJ intensity. Also, the direction of GPLLJ was usually southerly (Arritt et al. 1997; Bonner 1968; Mitchell et al. 1995). Based on that, the meridional wind was more crucial part of the GPLLJ.

	Zonal wind (m/s)	Meridional wind (m/s)	Precipitation (mm/12hours)
Daily	-1.94	3.95	2.24*
Nocturnal	-1.37	5.58	1.34
Daytime	-2.49	2.34	0.90

Table 3.3 Seasonal averages of area averaged WRF daily, nocturnal and daytime meridional wind, zonal wind and precipitation from May 1st to August 31st, 2002. The unit of daily precipitation (denote by "*") is mm/24hours.

	Zonal wind	Meridional wind	Precipitation
Daily	2.15	3.32	2.29
Nocturnal	2.75	3.71	1.55
Daytime	1.71	3.21	1.05

Table 3.4 Standard deviations of area averaged WRF daily, nocturnal and daytime meridional wind, zonal wind and precipitation from May 1st to August 31st, 2002.

From Figure 3.3, we can see the area averaged winds and rainfall exhibit similar features as in the NARR time series plot, both in seasonal variability and in diurnal cycles. The zonal winds in daily, nocturnal and daytime time period were much smaller than meridional winds. The GPLLJ was strongest in May and June. In July, strong GPLLJ events occurred less frequently and in August the number of strong GPLLJ increased again. In May and June, the direction and magnitude of meridional wind changed much faster than in July. Precipitation showed a more obvious diurnal cycle from WRF simulation than from NARR data. We can clearly see there were more strong precipitation events during the nocturnal hours. From the perspective of seasonal changes of precipitation, May and June were relatively wet, and July was relatively dry. In August, precipitation increased again.

From the above, it seems that the WRF captured the seasonal variability and diurnal cycles of the GPLLJ and precipitation quite well. Although the magnitudes of the GPLLJ and precipitation events were generally smaller in WRF than in NARR, WRF simulated the winds and rainfall well enough for our purpose.

To further validate the precipitation amount simulated by WRF, CPC rainfall data were used. One disadvantage of the CPC precipitation data is its time resolution: it only has daily accumulated values. Because of the importance of precipitation nocturnal peak, CPC rainfall data will have problems if we trying to use it as the analysis data for case selection and studies. We plotted the time series of area averaged daily CPC precipitation and compared with time series of area averaged daily NARR and WRF precipitation. We also plotted the daily precipitation for the U.S. to further validate NARR and WRF precipitation.

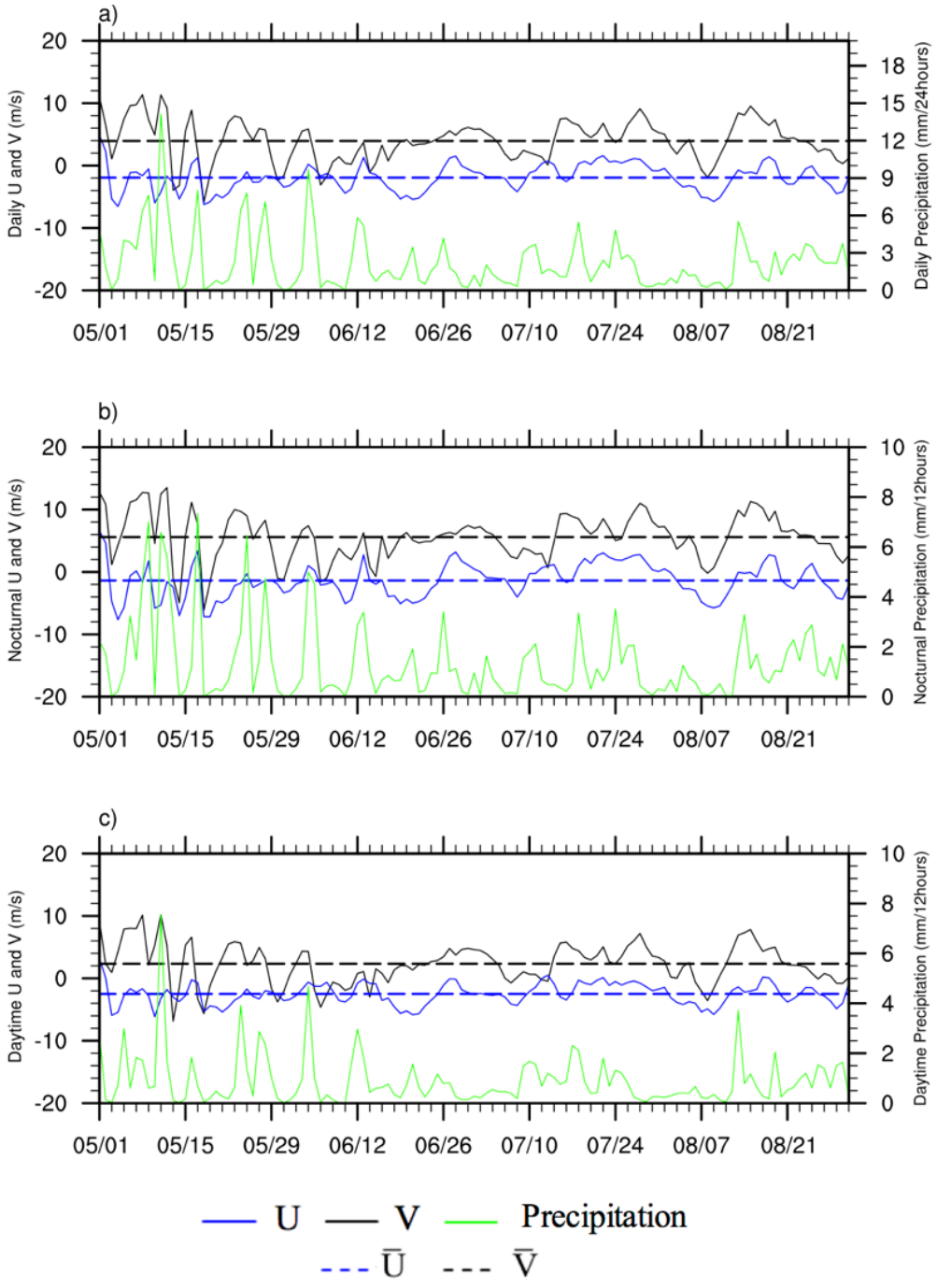

Figure 3.3 Time series of area averaged WRF 925 hPa U (zonal wind), V (meridional wind; 25-35°N, 102.5-92.5°W; units: m/s) and precipitation (35-45°N, 105-90°W; units: mm/24hours for a) and mm/12hours for b) and c)) of daily, nocturnal and daytime averages from May 1st to August 31st 2002. $\bar{U}$ and $\bar{V}$ are seasonal averages of U and V respectively. a), b) and c) shows daily, nocturnal and daytime U, V and precipitation respectively.

Figure 3.4 shows the time series of NARR, WRF and CPC rainfall. The data were calculated over the area (35-45°N, 105-90°W) from 00Z to 00Z of the next day for the comparison. The seasonal averages of precipitation of NARR, WRF and CPC were respectively are 2.79 mm/24hours, 2.24 mm/24hours and 2.54 mm/24hours. Compared to the interpolated observational rainfall data, NARR overestimated the seasonal averaged rainfall amount while WRF underestimated the amount. Judging by the standard deviation, NARR precipitation changed more frequently compared to WRF and CPC, while WRF precipitation was less than CPC.

Overall, the figure shows that WRF model simulation did a reasonably good job in simulating precipitation in the region of interest. In the first three months of warm season, 2002 (May, June and July), WRF simulated precipitation better than August. In May, June and July, NARR and WRF overestimated the amount of rainfall. In August, WRF tends to underestimate the magnitude of precipitation. However, it seems like WRF captured the seasonal changes of precipitation, judging by the area averaged precipitation information.

From the above, we conclude that the seasonal changes and values of winds and precipitation simulated by WRF, while not perfect, are sufficiently good that they can be used in the further analyses. However, the above validation is based on area averaged data. Area averaged data can show the magnitudes variables but not the spatial patterns of the variables. We want to make sure that WRF can also capture the spatial patterns of the GPLLJ and precipitation, which are essential for later study. To achieve that goal, we plotted daily 925 hPa winds and precipitation from May 1st to August 31st (figures not shown) to see if WRF simulated the basic spatial patterns of 925 hPa winds and

precipitation. After comparing the winds with NARR winds and precipitation with NARR and CPC data, it seems that although WRF may overestimate or underestimate the magnitudes of the GPLLJ and precipitation sometimes, it still simulated the structures relatively well.

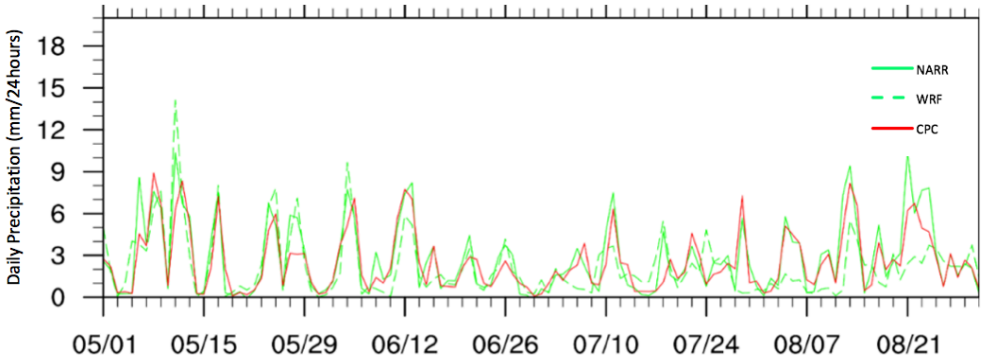

Figure 3.4 Time series of area averaged (35-45°N, 105-90°W) precipitation of NARR, WRF and CPC (units: mm/24 hours) from May 1st to August 31st, 2002. Green solid line denotes NARR precipitation; green dashed line denotes WRF precipitation and red solid line denotes CPC precipitation.

In conclusion, the data simulated by WRF is reasonable and can be used for the following analyses. In summary, for the warm season of 2002, WRF may overestimate the amount of rainfall of the time period from May to July while in August the amount may be underestimated. However, WRF captured the structures of the GPLLJ and precipitation as well as the nocturnal feature of precipitation.

Chapter 4

Model Results

4.1 Seasonal Variability of the GPLLJ and Synoptic Scale Settings

As mentioned in section 2.2, eventually we are going to focus on two case studies: one is from the "wet period" and another one from the "dry period" of the warm season. However, before that, we need some background information such as the seasonal variability of the GPLLJ, synoptic scale settings and moisture advection of each warm season month. In this way, we can get an idea of the overall role of GPLLJ and other factors in promoting warm season precipitation.

In the following sections, we show the seasonal variability of the GPLLJ (including seasonal changes of the GPLLJ's strength, frequency and path) and the relative roles of synoptic systems as well as moisture advection. By comparing the changes of the GPLLJ, synoptic systems activities and moisture advection, we anticipate they can help understand the differences between the "wet period" (May and June) and the "dry period" (July and August). However, as previous study pointed out (Wu and Raman 1998), on the basis of individual cases, it may be found out that the position and origins of the GPLLJ could affect its ability to transport moisture from the Gulf of Mexico and has less effects on warm season precipitation. That's one of the reasons we are going to study individual cases in the later section.

4.1.1 Seasonal variability of the GPLLJ

Figure 4.1 shows the monthly averaged 925 hPa wind speed and wind vectors from May to August, 2002. The blank area showed on Figure 4.1 is due to topography.

We can see the seasonal variability of the intensity and area of the GPLLJ. In May, the GPLLJ was the strongest among the entire warm season. The core of the GPLLJ was in the area of 30-35°N, 100-95°W. The magnitude of the GPLLJ decreased from late spring to early summer. In the area of the GPLLJ region we are interested in (25-35°N, 102.5-92.5°W), the maximum wind speed decreased from 12 m/s to about 9 m/s. Also, the core of the wind speed moved about 5° northward. In July, the wind speed was even smaller in the GPLLJ region compared to June. However, in August, the wind speed was larger than the wind speed of July. The area of strong wind speed also narrowed compared to extensive areas of strong GPLLJ in May and June. The core had a slightly smaller magnitude than in June. As expected, the strength of the GPLLJ was stronger in the "wet period" than "dry period". The trajectory of the GPLLJ overall was from south to north through May to June and stayed near for June, July and August.

The above shows the strength and path changes of the GPLLJ through the warm season. According to wind vectors plotted on Figure 4.1, we can see in the warm season of 2002, the monthly averaged winds are all southerly or southwesterly in the central U.S. In the core area of the GPLLJ, the wind direction was usually southerly. The wind circulation shows that the GPLLJ was likely transporting moisture from the Gulf of Mexico.

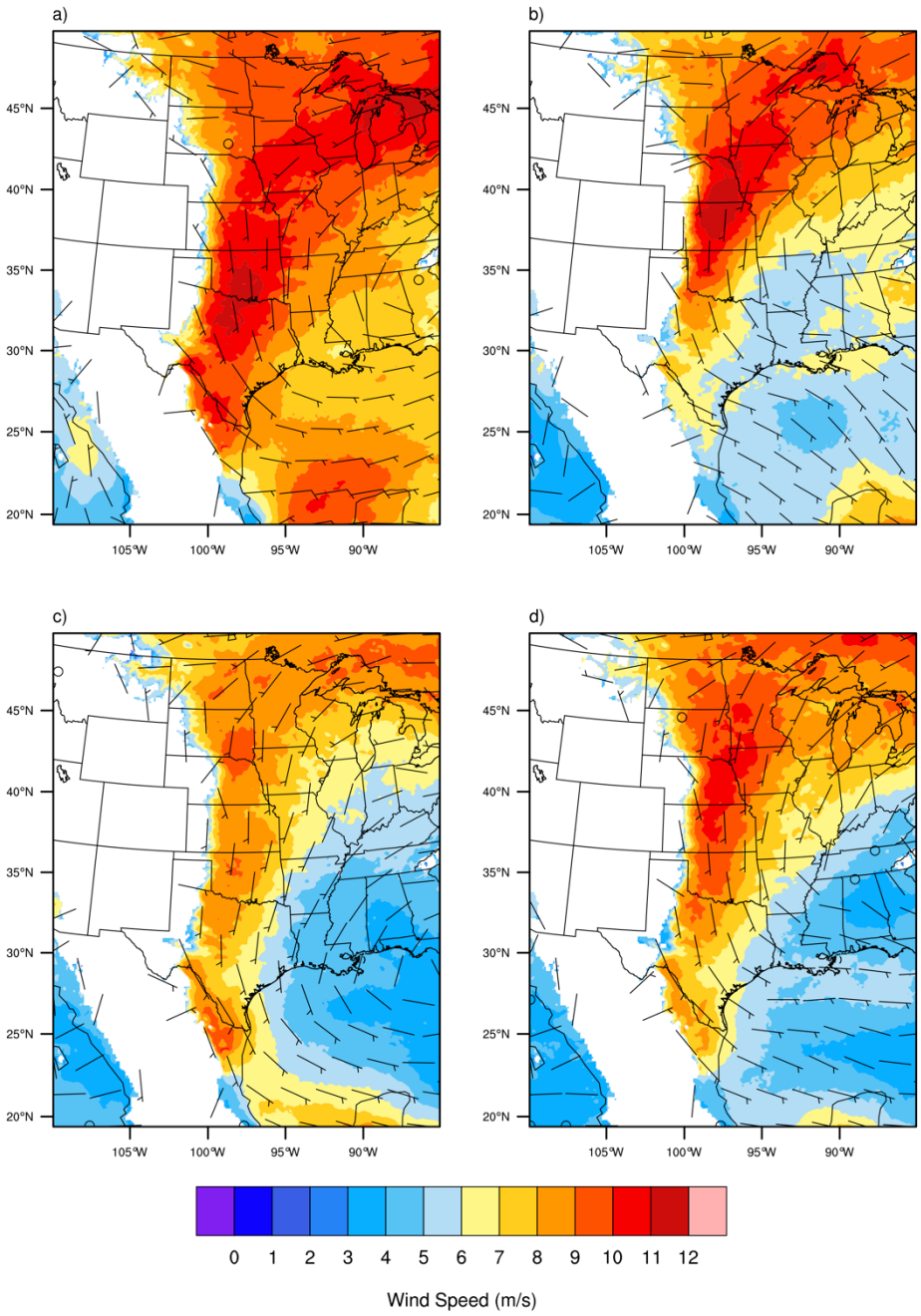

Figure 4.1 Monthly averages of 925 hPa wind speeds (shaded; units: m/s) and wind vectors (wind barb) from May to August, 2002. a) is monthly averages of May; b) is monthly averages of June; c) is monthly averages of July; d) is monthly averages of August.

We used the normalized standard deviation of 925 hPa wind speed to show the frequency changes of the GPLLJ, as plotted in Figure 4.2. The blanks in Figure 4.2 were due to the topography as well. The equation we used to do this normalization process is

$$Z = \frac{\sigma}{\sigma_{max}} \tag{4.1}$$

where σ is standard deviation of each month and σ_{max} is maximum of standard deviation of each month. From Figure 4.2 we can see the frequency of the GPLLJ activities is highest in May, focused on 30°-40°N, 100°-95°W in the central U.S. In June and August, the area of high frequency GPLLJ activities moved northeastward compared to May, about 40°-45°N, 97°-90°W. In July the position of high frequency GPLLJ activities core is similar to May but was less frequent.

To sum up, the GPLLJ is more active (both from strength and frequency aspects) in the "wet period" than "dry period" with position more to the south in May (about 5°). The monthly averaged wind directions for the interested areas fell into the range between south and southwest. Monthly averaged data only provide background information of the GPLLJ activities through the whole season.

4.1.2 Seasonal Variability of Synoptic Scale Settings

It is clear that the presence and strength of synoptic scale systems are very important for the development of precipitation in the study region. We are interested in finding the mechanisms of how the GPLLJ interacted with synoptic systems. We used eddy kinetic energy (EKE) to show the activities of synoptic systems.

The equation for calculating eddy growth rate is

$$\text{EKE} = \int_{1000\ hPa}^{200\ hPa} \{\frac{1}{2} \times [(U')^2 + (V')^2]\} dp \tag{4.2}$$

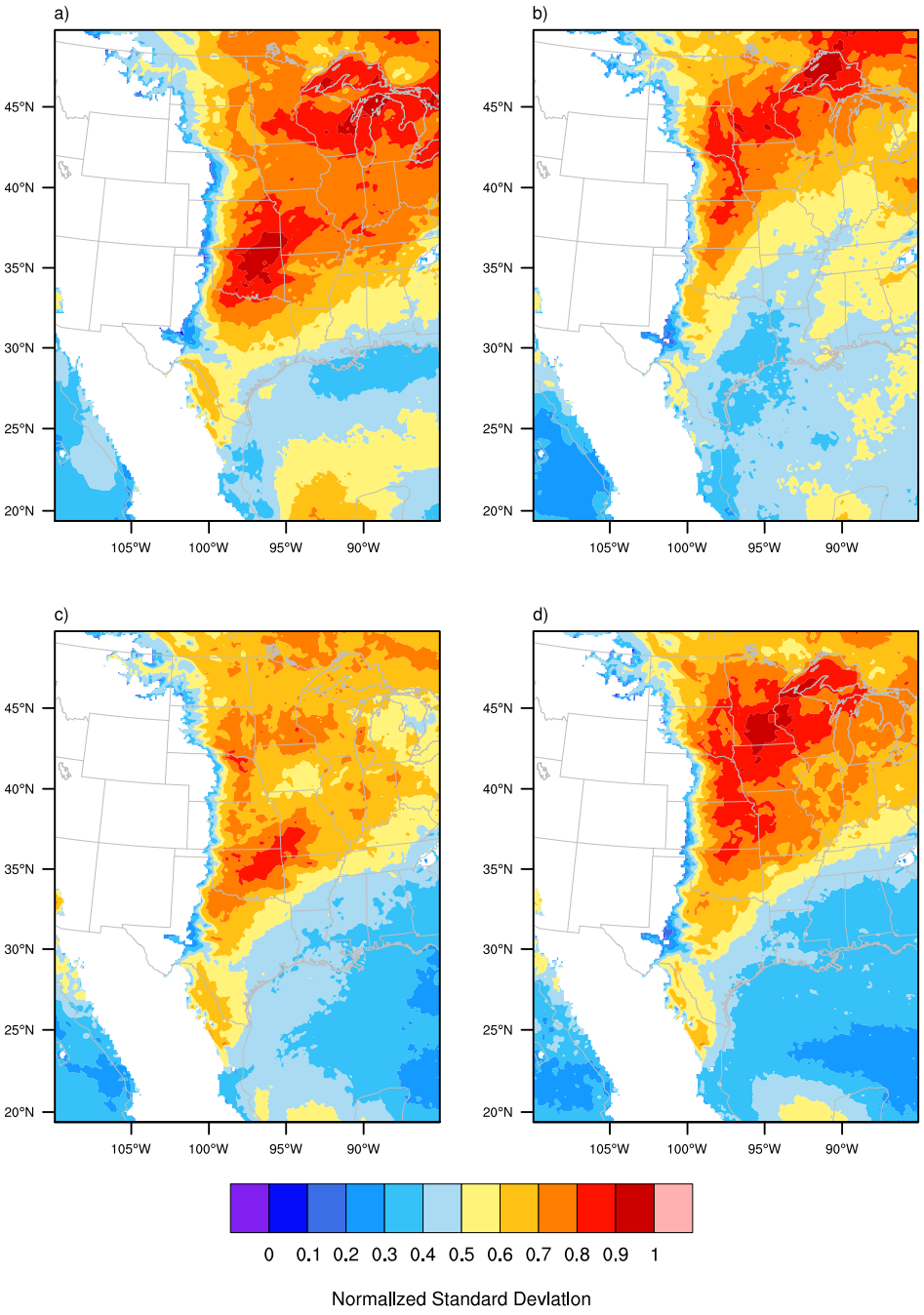

Figure 4.2 Monthly averages of normalized standard deviation of 925 hPa wind speeds from May to August, 2002. a) is monthly averages of May; b) is monthly averages of June; c) is monthly averages of July; d) is monthly averages of August.

where U' and V' are anomaly departures from the entire season of zonal and meridional winds. We calculated the vertically integrated EKE from 1000 hPa to 200 hPa. Also, to focus on the activities of synoptic systems, we processed the EKE results with band-pass filter and retain the systems with a time scale range of 2-6 days. The monthly averages of running average of filtered EKE and precipitation are shown in Figure 4.3. The structures of monthly averaged precipitation indicate that springtime (May and June) was the "wet period". The precipitation in May occurred in the area of 35°-45°N, 100°-90°W, at the northern nose of the GPLLJ area. The large precipitation in June showed up in further northeastward. Compared to springtime, summertime (July and August) didn't have large overall precipitation in the central U.S., referred as the "dry period". Judging by the position of the precipitation, precipitation in wet period might closely relate to moisture transported by the GPLLJ because it occurs at the nose of the GPLLJ. However, from the "dry period", even though the GPLLJ became more active in August, there was no outstanding precipitation over the Great Plains area. The absence of precipitation might be caused by the reduced impact of large-scale synoptic forcing.

From Figure 4.3, it is clear that the EKE was highest in May with a maximum value of 2×10^5 J/m^2. The number decreased in the following three months to 1.2×10^5 J/m^2, 0.8×10^5 J/m^2 and 0.8×10^5 J/m^2 respectively. This indicated that synoptic systems were the most active in May, then weakened in June, July and August. The precipitation occurred in the edge of a high EKE core in May. In June, precipitation usually occurred near the center of a high EKE core. In July and August, relatively low EKE and less precipitation amount indicates the reduced impact of 2-6 days' time scale synoptic systems.

4.2 Seasonal Variability of Moisture Advection

Moisture advection is one of the most significant effects of the GPLLJ on precipitation. The seasonal variability of moisture advection can help understand the moisture environment differences between the "wet period" and the "dry period".

Because the magnitude of meridional wind is larger than zonal wind, we only used moisture advection by meridional wind to show the moisture situation of the warm season. The moisture advection was calculated using the following equation

$$Q = \int_{1000\ hPa}^{700\ hPa} (q \times v) dp \tag{4.3}$$

where q is the water mixing ratio and v is meridional wind. The moisture advection was integrated from 1000 hPa (taken as the surface for this situation) to 700 hPa, for the moisture advection usually concentrated on pressure levels under 700 hPa (Helfand and Schubert 1995).

From Figure 4.4, it seems like the maximum monthly averages of moisture advection by meridional wind were similar from May to August. However, the position of the moisture advection core varied through the warm season. In May, the core of moisture advection was in the area of 25-35°N, 102.5-92.5°W, similar to the core of the GPLLJ. The position of moisture advection core moved about 5° northward in June. The coincidence in path change of moisture advection and the wind circulation implies that during the "wet period", the GPLLJ transported moist air from the Gulf of Mexico to the central U.S. The moist environment created by the GPLLJ was favorable for inducing rainfall. The key question becomes what was the lifting mechanism. In July, with weakened GPLLJ activities, the magnitude of moisture advection by meridional wind was close to the former two months. That means in July, the water vapor mixing ratio was

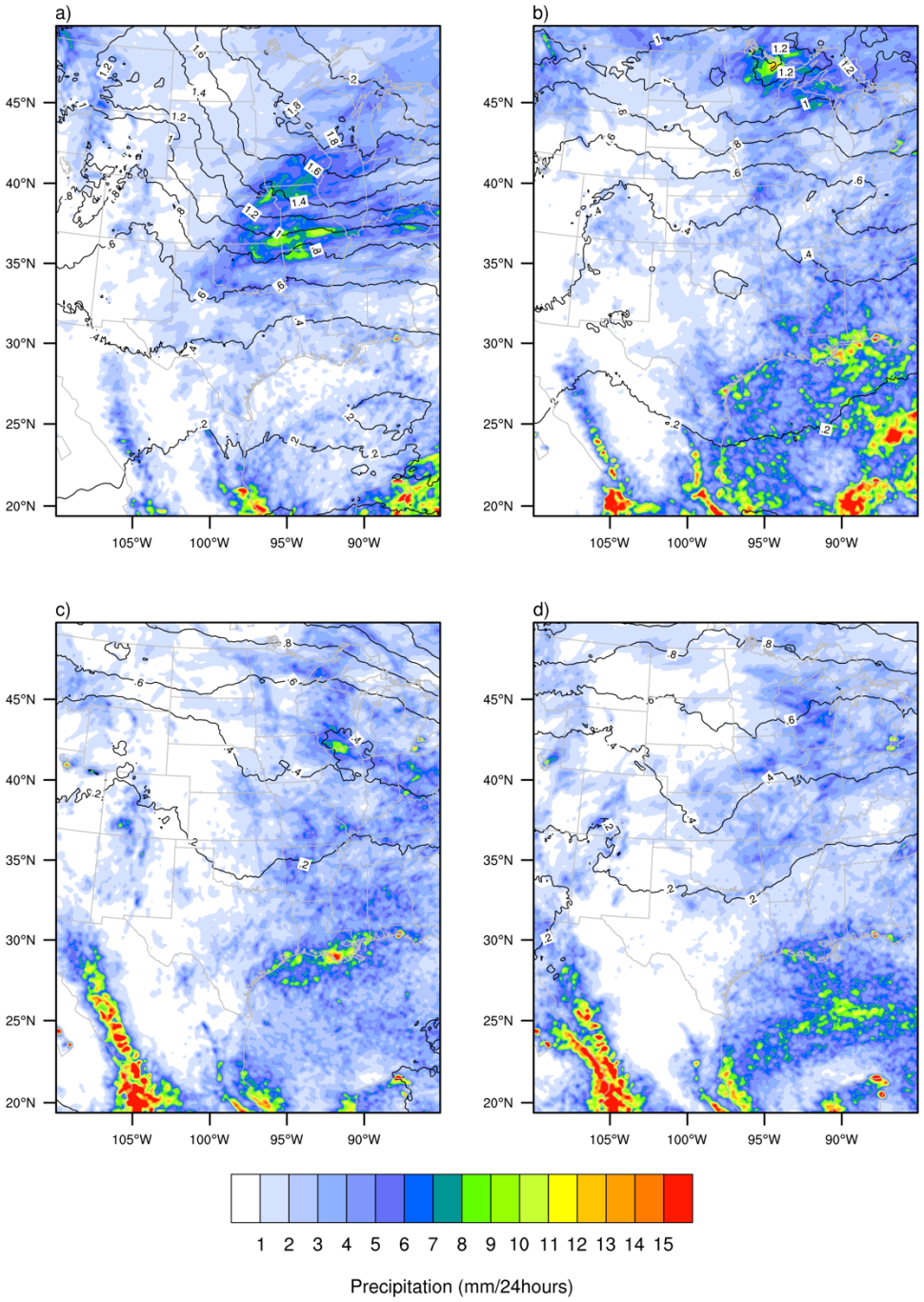

Figure 4.3 Monthly averages of precipitation (shaded, unit: mm/24hours) and band-pass filtered eddy kinetic energy (contoured, unit: 10^5 J/m^2) from May to August, 2002. a) is monthly averages of May; b) is monthly averages of June; c) is monthly averages of July; d) is monthly averages of August.

higher than in the “wet period”. That is because in summer, the overall warmer atmosphere can hold more water. However, the position of moisture advection core was in southern Texas, indicating that in July, moisture might not be transported into the precipitation area we are interested in. By August, the moisture advection moved northward again compared to July, similar to the path of the GPLLJ in August as well. However, even with ample moisture in July, the lack of rising motion led to absence of precipitation (McCorcle 1988; Wu and Raman 1998).

Through the above analysis, it seems like in the “wet period”, the GPLLJ activities were closely related to moisture transport into interested rainfall area while in the “dry period”. For example, in July, the weakened GPLLJ indicated decreased meridional velocity. However, the moisture advection in July was much stronger meaning increased water vapor mixing ratio. Judging by equation (4.3), the weakened GPLLJ in July still transported ample moisture. Considering moisture advection, although the path was similar to the trajectory of the GPLLJ, the magnitude didn’t change as much as the strength of GPLLJ through the warm season. In the next section, we will compare the synoptic systems settings of these two time periods.

In conclusion, for the “wet period”, the GPLLJ was more active, in strength and frequency. Large precipitation events tended to show up at the northern nose of the GPLLJ. Also, there were more effects of synoptic systems during the wet period. For the “dry period”, there were fewer and weaker GPLLJ events, with less obvious precipitation cores. The filtered EKE indicates less effect on precipitation from 2-6 days’ scale synoptic systems. Overall, in the “wet period”, the atmosphere was more energetic than in the dry period. The maximum magnitudes and trajectory of moisture advection and

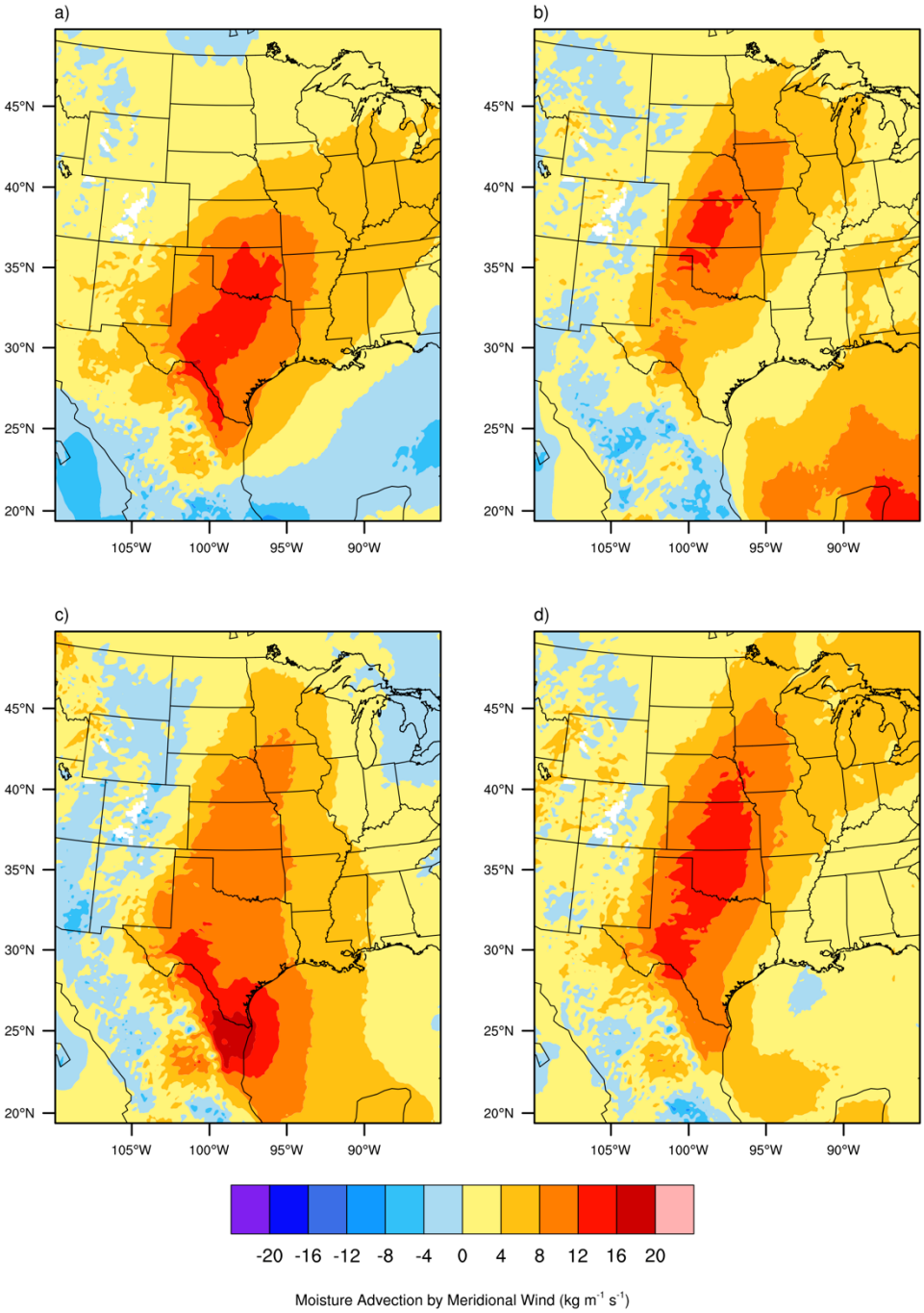

Figure 4.4 Monthly averages of moisture advection by meridional wind integrated from 1000 hPa to 700 hPa (unit: kg m^{-1} s^{-1}) from May to August, 2002. a) is monthly averages of May; b) is monthly averages of June; c) is monthly averages of July; d) is monthly averages of August.

trajectory was similar over the entire warm season. In the below analysis, we select two cases to compare different mechanisms of how the GPLLJ contributed to precipitation.

4.3 Case Selections and Studies

After comparing differences of the GPLLJ, synoptic scale settings and moisture advection during the two periods, two cases were selected for further analysis. For the case selection, one important criterion is the presence of the GPLLJ and precipitation activity. We also tried to avoid high EKE around the precipitation area, to better determine the actual roles of the GPLLJ played in promoting precipitation. After going through 6 hourly winds, precipitation and EKE plotting (figures not shown), two cases from different time periods were selected. One is the precipitation case around May 24th, from the "wet period" and the other one around July, 19th, from the "dry period". Both of the cases have low EKE around the precipitation areas, which can be considered as indicating relatively less effect from synoptic systems.

To show the evolution of the GPLLJ in those two cases, we plot the area averaged meridional wind, representing the strength of the GPLLJ, from May 19th to May 29th for the first case and from July 14th to July 24th for the second case in Figure 4.5. The vertical levels were interpolated from 1000 hPa to 500 hPa with an interval of 10 hPa.

From Figure 4.5, we can see the strength of the GPLLJ was slightly stronger in the first case than in the second case. Both cases showed clear diurnal cycles: the meridional wind reached peak around 06Z every day and weakened during the daytime. It seems like the peak meridional wind speed lasted a little longer in May case than in July case. Judging by the strength and durations, overall the GPLLJ was a little more active in

May case. The precipitation occurred when the GPLLJ reached mature stages in the May case. However, in the July case, the precipitation occurred when the GPLLJ started to weaken. The different occurrence times in those two cases may indicate the mechanisms of the GPLLJ inducing precipitation were different. On the account of the GPLLJ core often occurred around 925 hPa for both cases, we continued to use 925 hPa winds to show the activities of the GPLLJ.

In the case studies, we will focus on how the GPLLJ interacted with different processes on different scales to produce precipitation. On the basis of the development of precipitation, the first case was from May 22nd to May 26th and the second case was from July 17th to 19th.

Figure 4.6 shows the winds, geopotential height and divergence at 925 hPa as well as precipitation from May 22nd to May 26th. From Figure 4.6, we can see in the first case, precipitation stared to occur in May 23rd (Figure 4.6b), developed and matured in May 24th (Figure 4.6c) and May 25th (Figure 4.6d). By May 26th (Figure 4.6e), precipitation dissipated. In this case, the diurnal cycle of precipitation was similar during the whole process: developed in the late afternoon (00Z), reached its peak around midnight (06Z) then dissipated in the daytime (represented by 12Z and 18Z). Around May 24th, a wind boundary formed in the area of 35°-40°N, 100°-95°W in the middle of the night. To the south of the boundary, the wind direction was southwest, while north of the boundary, the wind direction was northeast. The position of the wind boundary and precipitation were very close. The development of the GPLLJ was one day earlier than the appearance of precipitation. Around midnight of May 22nd, there was a strong southerly wind flow from Texas to Nebraska. The GPLLJ intensified on May 23rd then weakened in

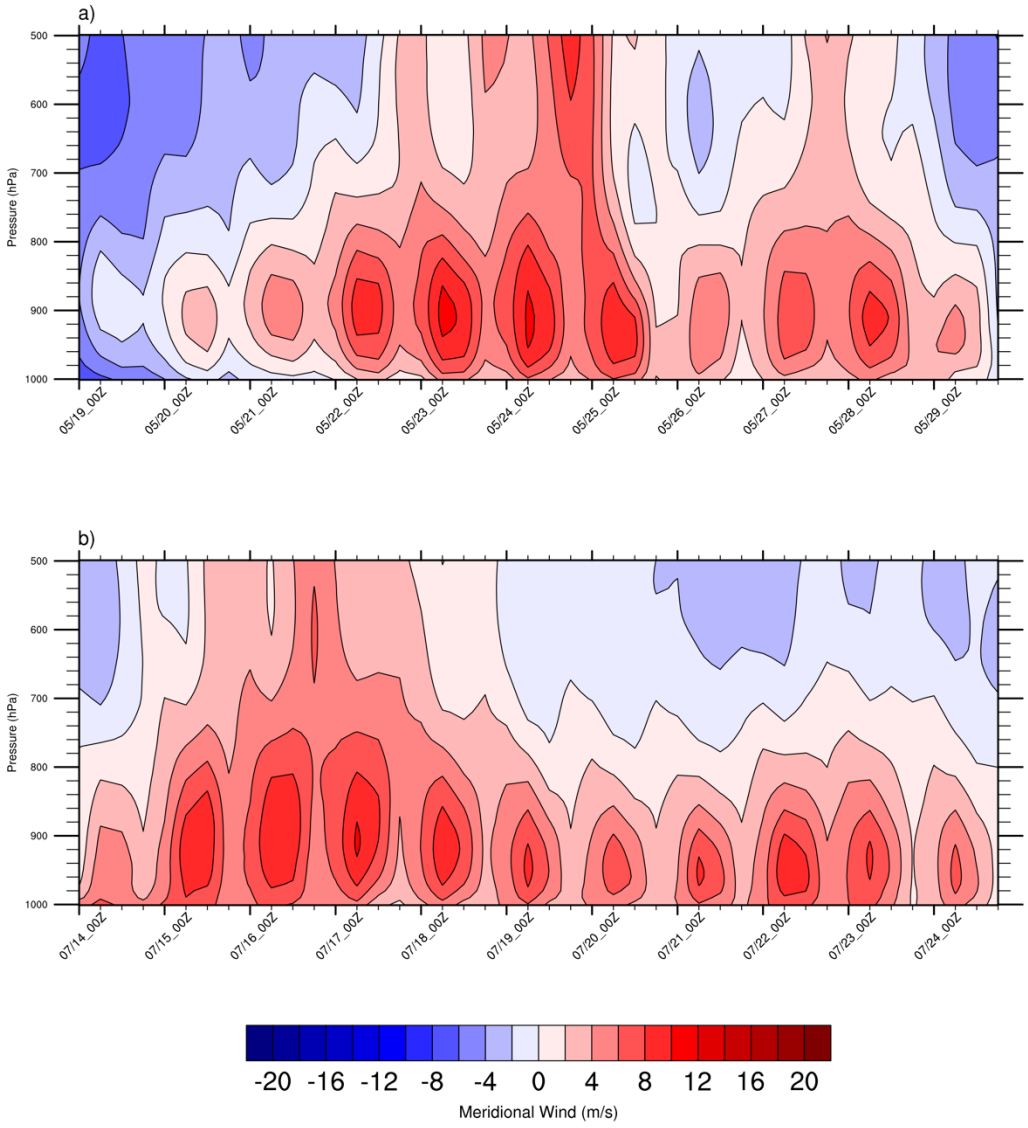

Figure 4.5 Area averages of meridional wind on different levels for two selected cases. a) is from May 19th to May 29th; b) is from July 14th to July 24th.

May 24th and 25th. In May 26th, there was no obvious GPLLJ activity. The diurnal cycle of the GPLLJ was similar to the diurnal cycle of precipitation: maximum wind speed occurred around midnight and decreased in the daytime.

(a)

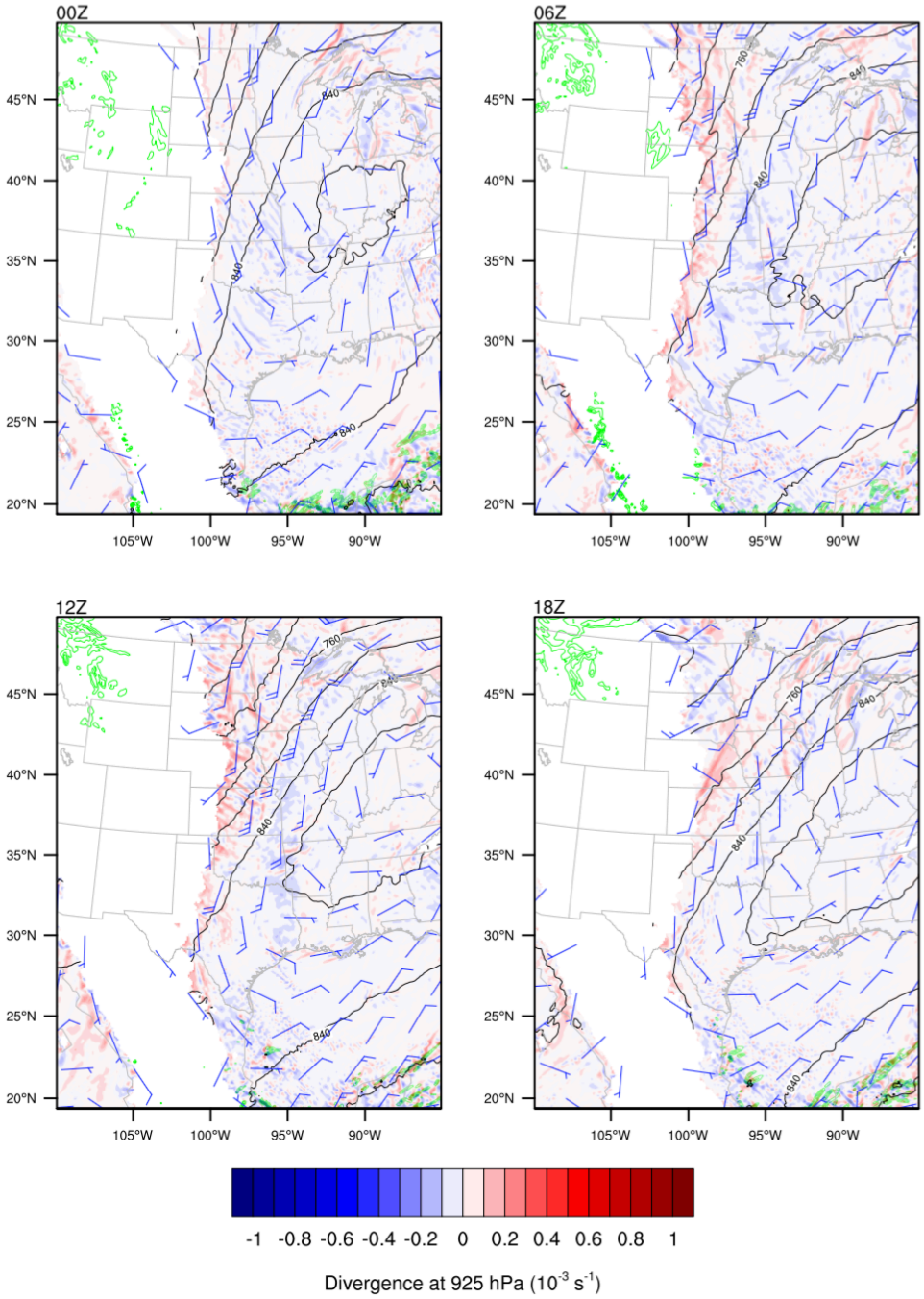
00Z
06Z
12Z
18Z
45°N
40°N
35°N
30°N
25°N
20°N
105°W
100°W
95°W
90°W
760
840
-1 -0.8 -0.6 -0.4 -0.2 0 0.2 0.4 0.6 0.8 1
Divergence at 925 hPa (10^-3 s^-1)

(b)

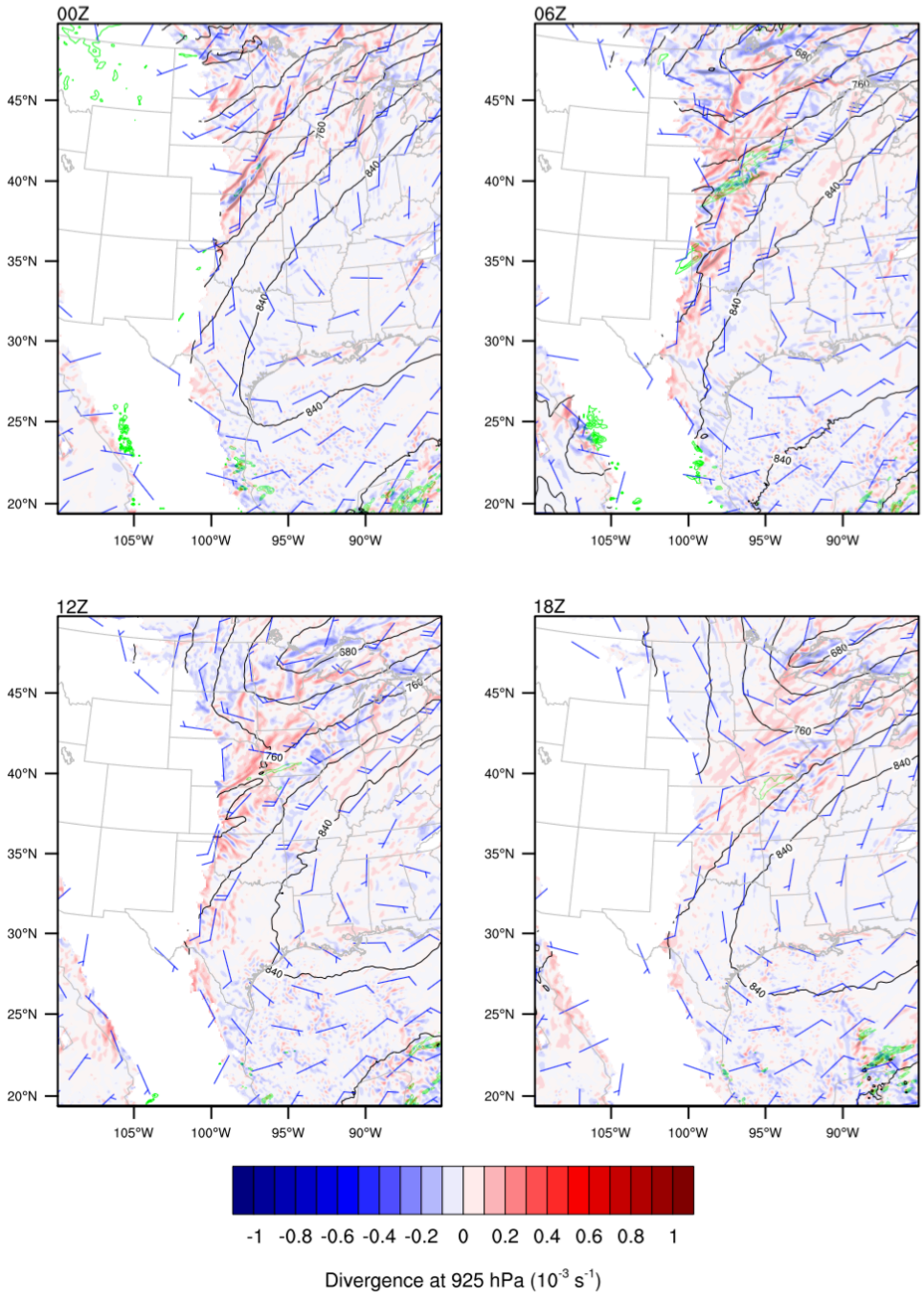
00Z
06Z
12Z
18Z
45°N
40°N
35°N
30°N
25°N
20°N
105°W
100°W
95°W
90°W
580
680
760
840
-1 -0.8 -0.6 -0.4 -0.2 0 0.2 0.4 0.6 0.8 1
Divergence at 925 hPa (10^-3 s^-1)

(c)

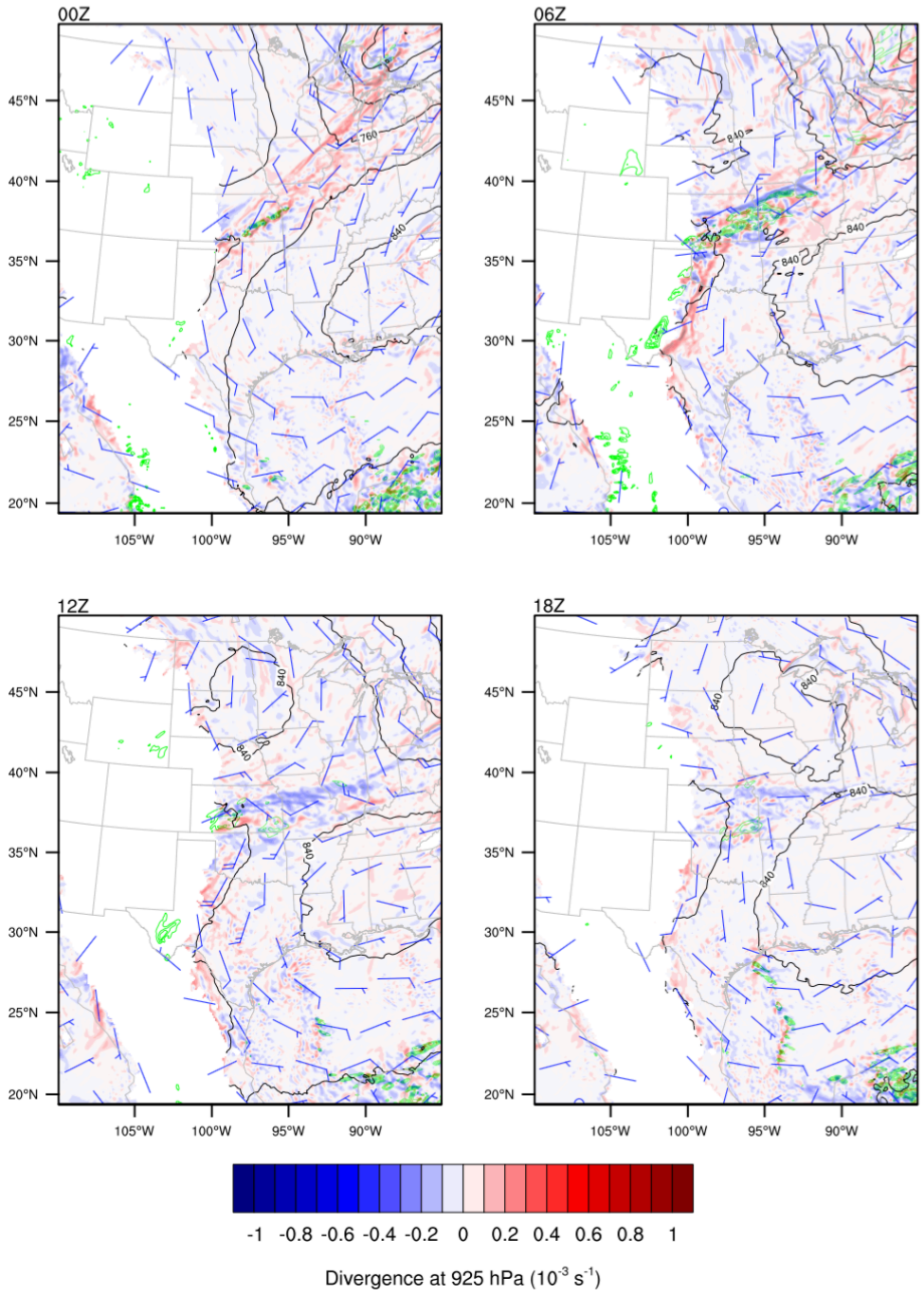
00Z
06Z
12Z
18Z
45°N
40°N
35°N
30°N
25°N
20°N
105°W
100°W
95°W
90°W
760
840
-1 -0.8 -0.6 -0.4 -0.2 0 0.2 0.4 0.6 0.8 1
Divergence at 925 hPa (10^-3 s^-1)

(d)

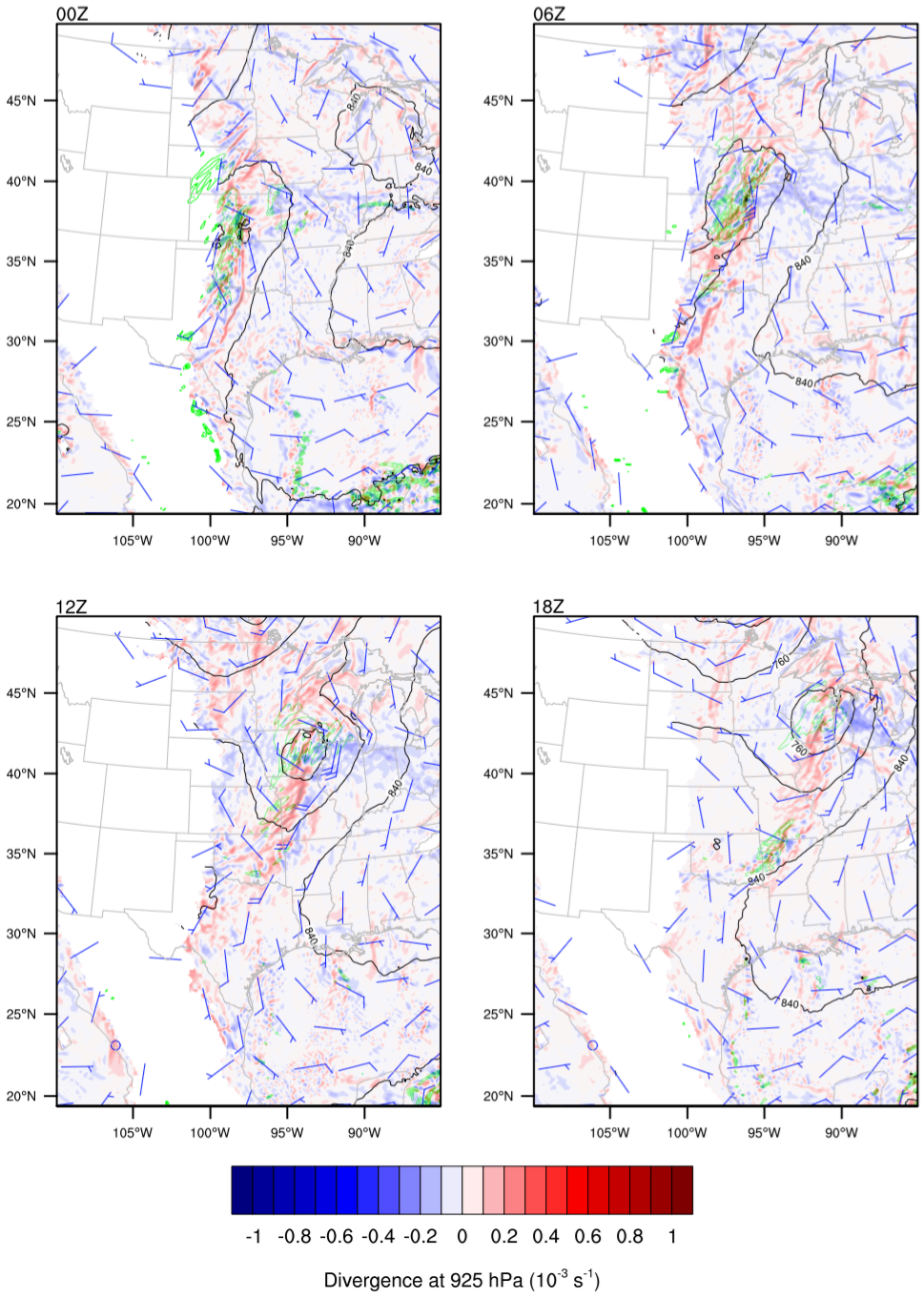
00Z
06Z
12Z
18Z
45°N
40°N
35°N
30°N
25°N
20°N
105°W
100°W
95°W
90°W
840
-1 -0.8 -0.6 -0.4 -0.2 0 0.2 0.4 0.6 0.8 1
Divergence at 925 hPa (10-3 s-1)

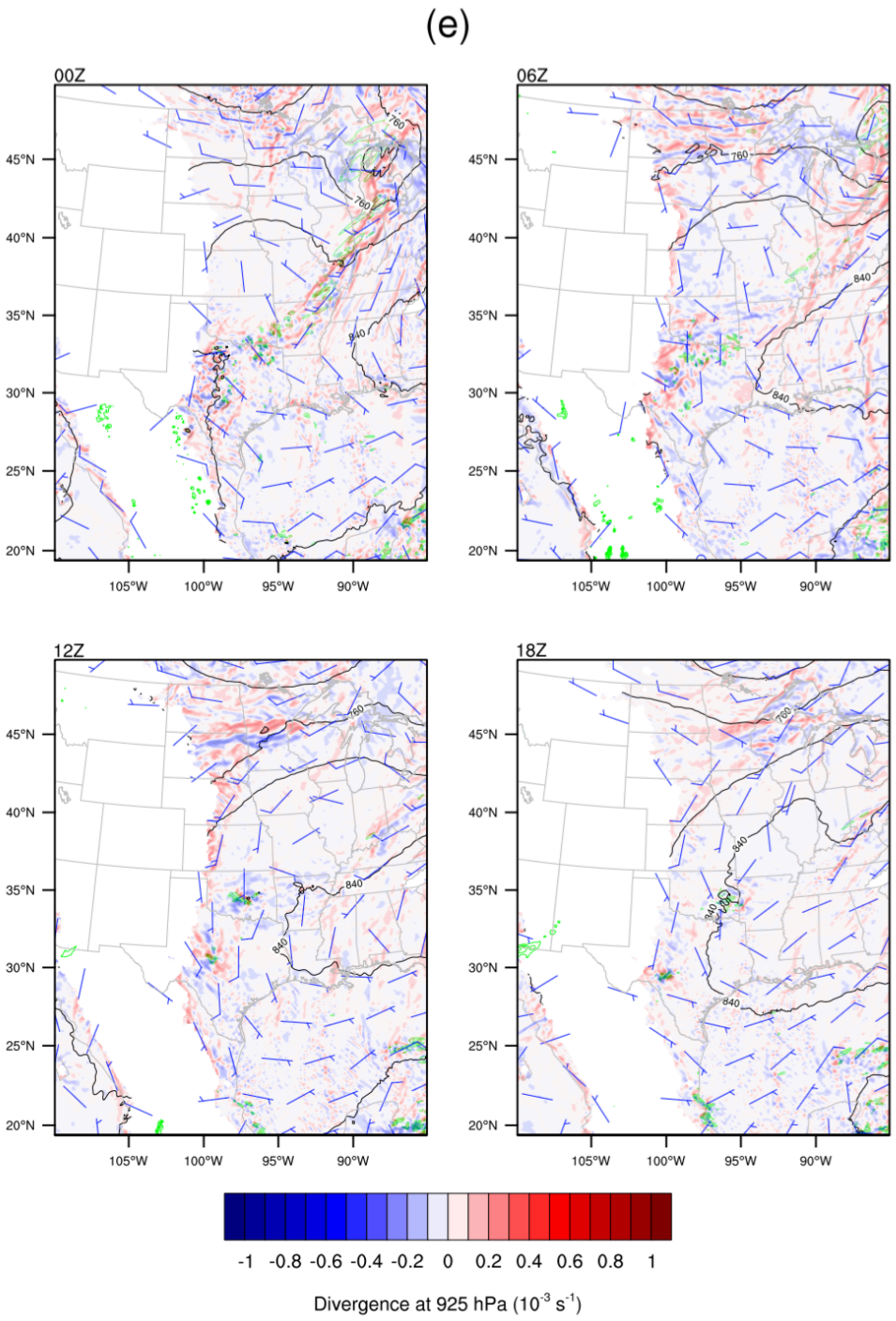

Figure 4.6 6 hourly Winds (vector, unit: knots), geopotential height (black contour, unit: m) and divergence (shaded, unit: 10^{-3} s^{-1}) at 925 hPa and precipitation (green contour, contoured from 0 mm/6hours to 60 mm/6hours by 10 mm/6hours, unit: mm/6hours) from May 22nd to 26th, 2002. (a) is May 22nd; (b) is May 23rd; (c) is May 24th; (d) is May 25th and (e) is May 26th.

Figure 4.7 shows the winds, geopotential height and divergence at 200 hPa, as well as precipitation. From Figure 4.7, we can see that there was a westerly upper-level jet in the area from northern New Mexico to Wyoming from May 22nd to May 24th (Figure 4.7a-c) and the central U.S. was under the influence of a short wave trough. The trough kept developing until May 25th (Figure 4.7d). At the same time, the westerly upper-level jet axis moved eastward at a slow pace, with the central U.S. in the exit area of the upper-level jet streak. From May 25th, the trough weakened considerably and the upper-level wind direction changed from southwest to northwest, indicating the central U.S. wasn't in the upper-level jet exit region anymore.

Combining the results shown in Figure 4.6 and Figure 4.7, the position of the GPLLJ was often embedded below the exit region of the upper-level jet. The relationship of this position pattern was related to possible effects of upper-level jet streak on the formation of the GPLLJ proposed by Uccellini (1979). In this study, a hybrid isentropic and sigma coordinate numerical model was used to study the mass and momentum adjustments between upper and lower-level jet streaks. The mass adjustment is a two-layer pattern: in the upper-level jet exit region, the air decelerates and leads to an ageostrophic component of the wind with direction to the anticyclonic side. For that reason, there is mass divergence in the cyclonic area, which needs to be compensated by the lower-level mass convergence. The replenished mass from the lower-level caused an isallobaric wind, which is a primary factor for the development of the GPLLJ (Uccellini and Johnson 1979).

(a)

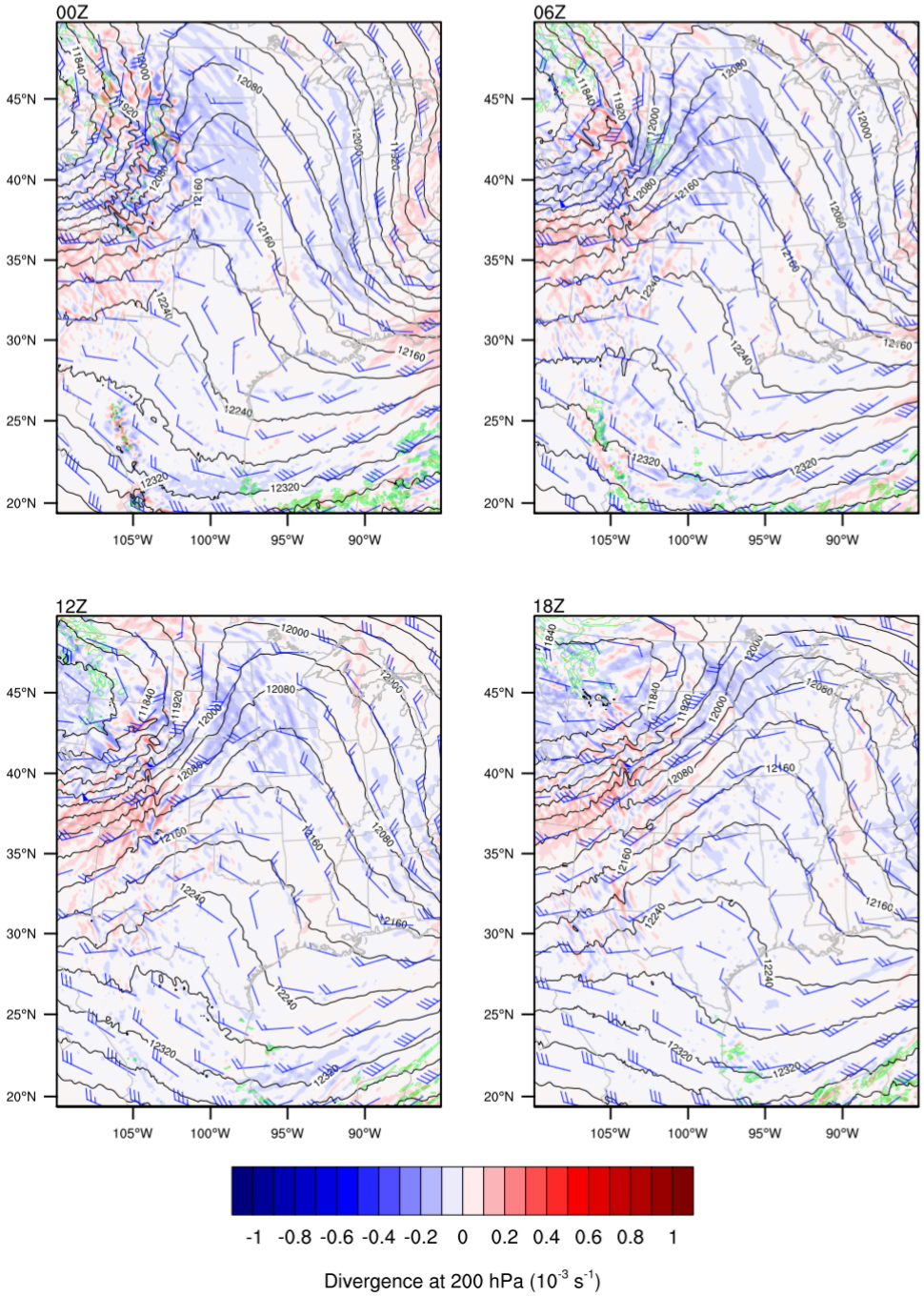
00Z
06Z
12Z
18Z
45°N
40°N
35°N
30°N
25°N
20°N
105°W
100°W
95°W
90°W
-1 -0.8 -0.6 -0.4 -0.2 0 0.2 0.4 0.6 0.8 1
Divergence at 200 hPa (10-3 s-1)

(b)

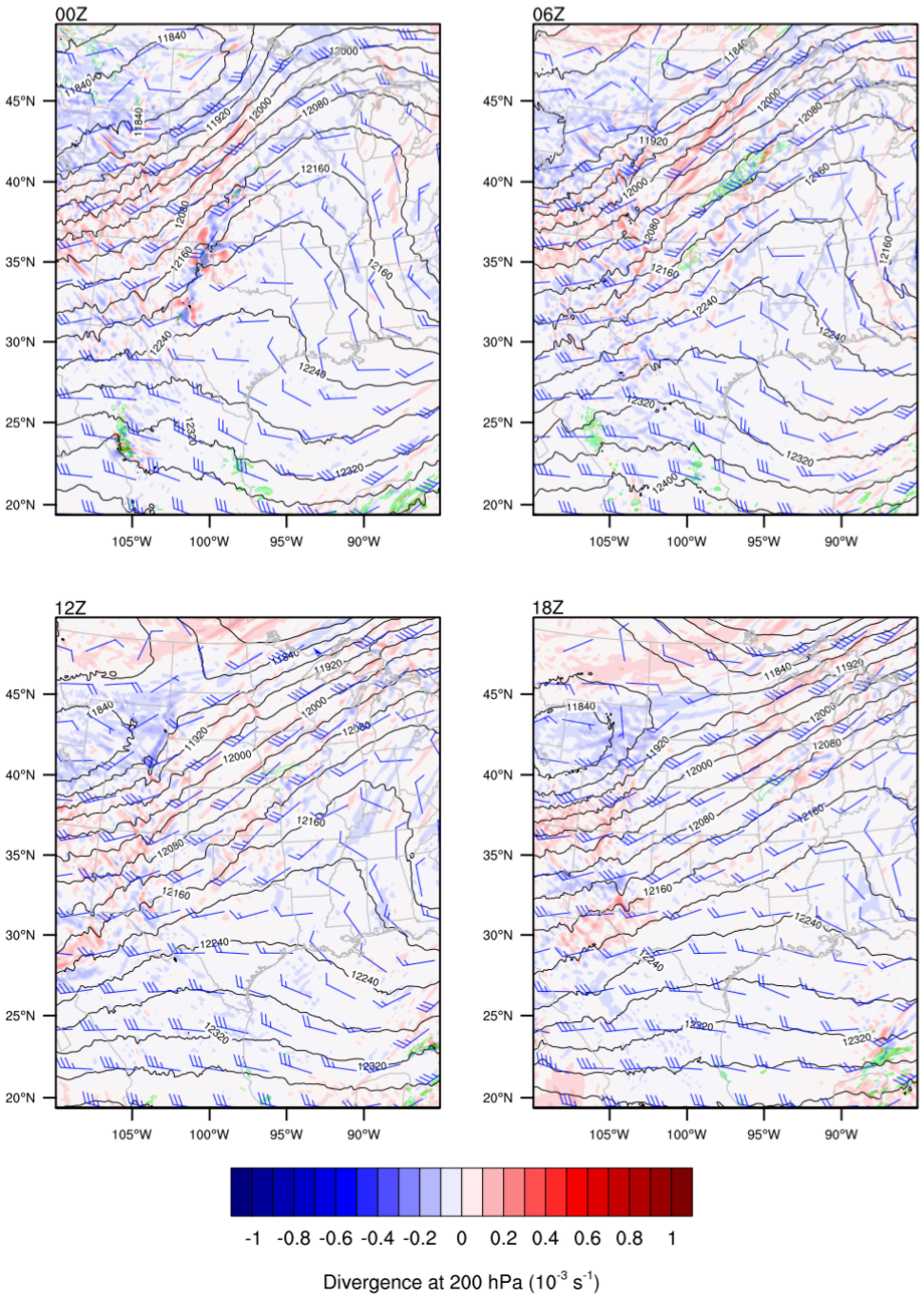
00Z
06Z
12Z
18Z
45°N
40°N
35°N
30°N
25°N
20°N
105°W
100°W
95°W
90°W
-1 -0.8 -0.6 -0.4 -0.2 0 0.2 0.4 0.6 0.8 1
Divergence at 200 hPa (10-3 s-1)

(c)

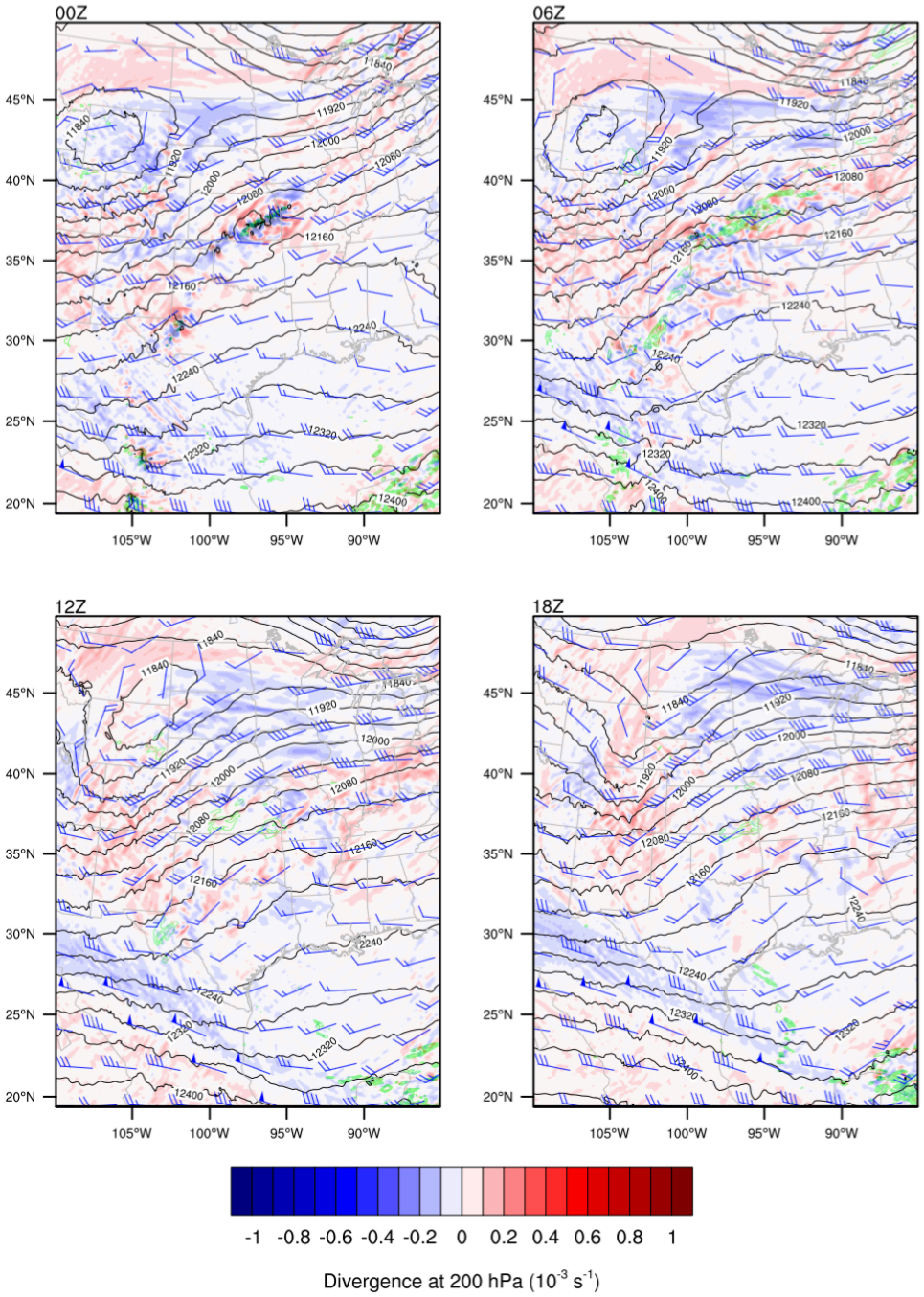
00Z
06Z
12Z
18Z
45°N
40°N
35°N
30°N
25°N
20°N
105°W
100°W
95°W
90°W
-1 -0.8 -0.6 -0.4 -0.2 0 0.2 0.4 0.6 0.8 1
Divergence at 200 hPa (10-3 s-1)

(d)

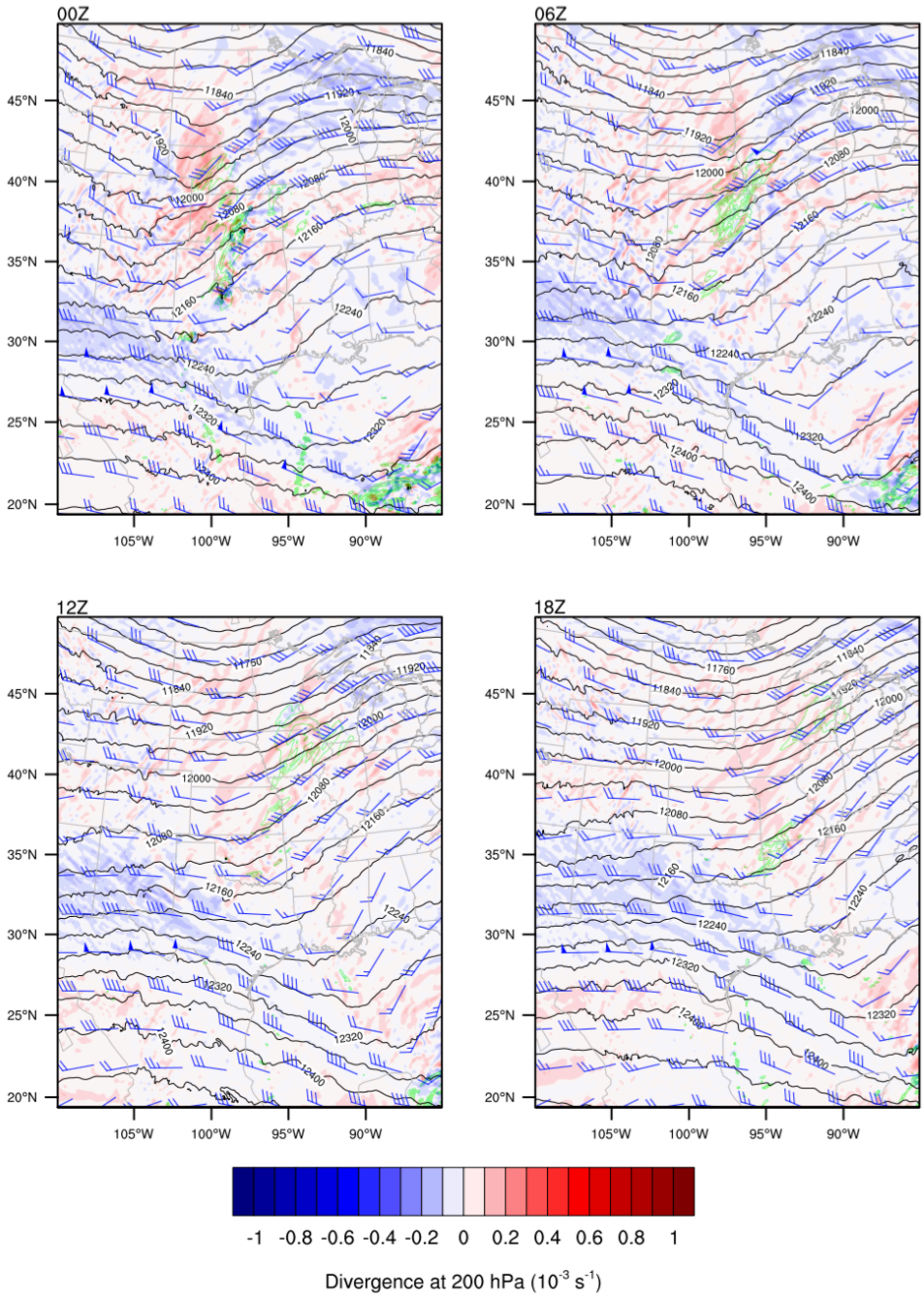
00Z
06Z
12Z
18Z
45°N
40°N
35°N
30°N
25°N
20°N
105°W
100°W
95°W
90°W
-1 -0.8 -0.6 -0.4 -0.2 0 0.2 0.4 0.6 0.8 1
Divergence at 200 hPa (10-3 s-1)

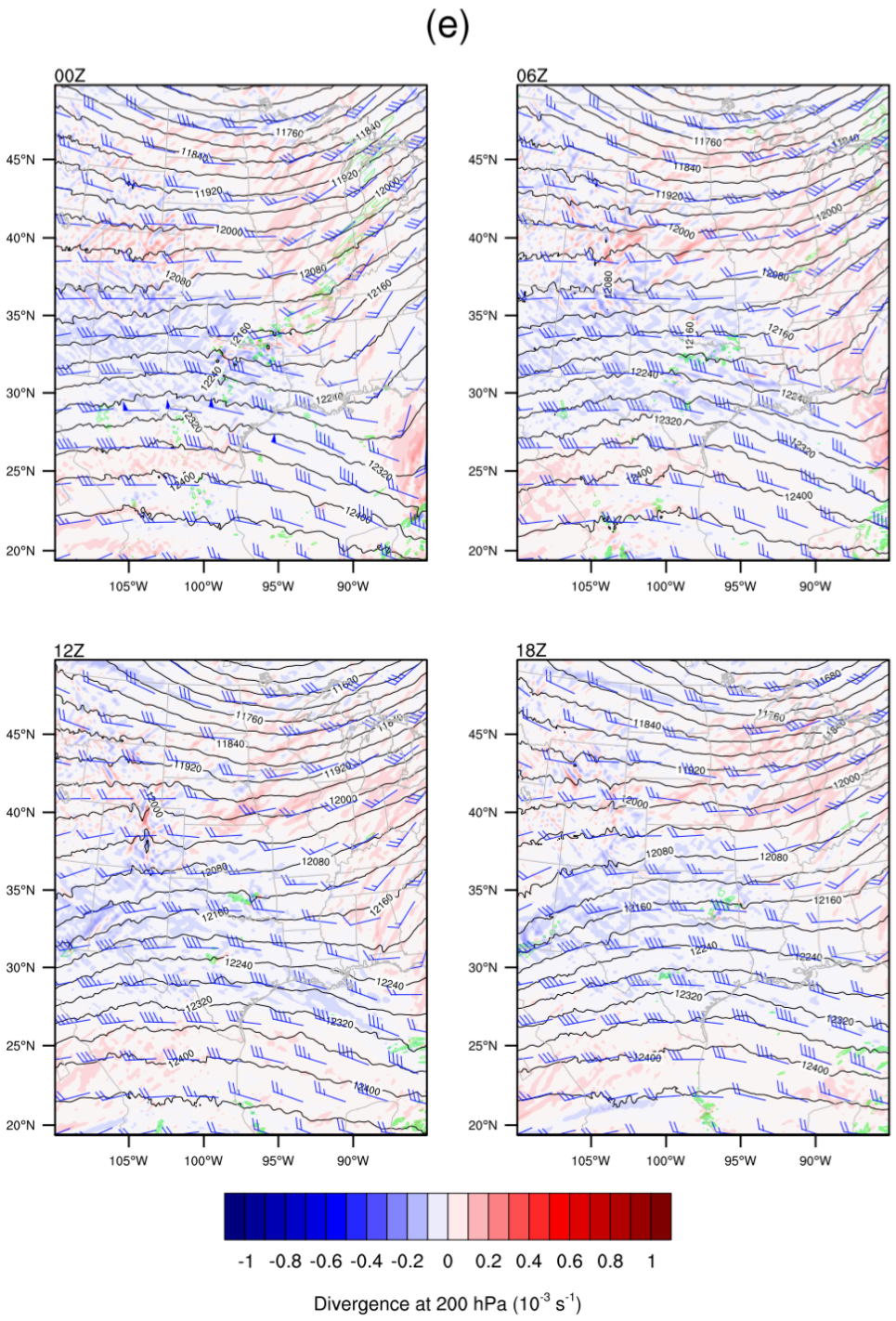

Figure 4.7 6 hourly winds (vector, unit: knots), geopotential height (black contour, unit: m) and divergence (shaded, unit: 10^{-3} s^{-1}) at 200 hPa and precipitation (green contour, contoured from 0 mm/6hours to 60 mm/6hours by 10 mm/6hours, unit: mm/6hours) from May 22nd to 26th, 2002. (a) is May 22nd; (b) is May 23rd; (c) is May 24th; (d) is May 25th and (e) is May 26th.

The mechanism in the first case can be explained well by the dynamic process described above. From Figure 4.7, it seems in the upper-level jet exit region, there was divergence along the northern boundary of precipitation. From Figure 4.6, we can see that low-level convergence occurred in the similar area of upper-level divergence. The occurrence of convergence in the lower level can be explained by the two-layer mass adjustment. This also indicated that the propagation of upper-level jet streak resulted in the lower-level convergence as well as the formation of the GPLLJ in this case. The coupling of upper-level divergence and lower-level convergence caused rising motion. After the formation of the GPLLJ, it transported warm, moist air from the Gulf of Mexico. Combined with the rising motion, precipitation was produced at the northern region of the GPLLJ.

Figure 4.8 shows the vertical cross sections of winds, equivalent potential temperature and water vapor mixing ratio perpendicular to the precipitation line (from 35°N, 100°W to 40°N, 95°W). On Figure 4.8, the precipitation area itself was represented by 37°N, 97°W. When the GPLLJ occurred, it transported warm, moist air from the Gulf of Mexico into the precipitation area, with the water vapor mixing ratio and equivalent potential temperature both increasing around the precipitation area from May 22nd (Figure 4.8a). In May 24th (Figure 4.8c), a dryline was formed along southwest to northeast. The low-level (925 hPa) wind direction in the north of the dryline was northeast, while in the south of the dryline the low-level wind direction was southeast. After the dryline was formed, there was a clear moisture boundary around the precipitation area. Judging by the equivalent potential temperature and water vapor mixing ratio, the GPLLJ also contributed to the development of precipitation by bringing moisture in and destabilizing the atmosphere.

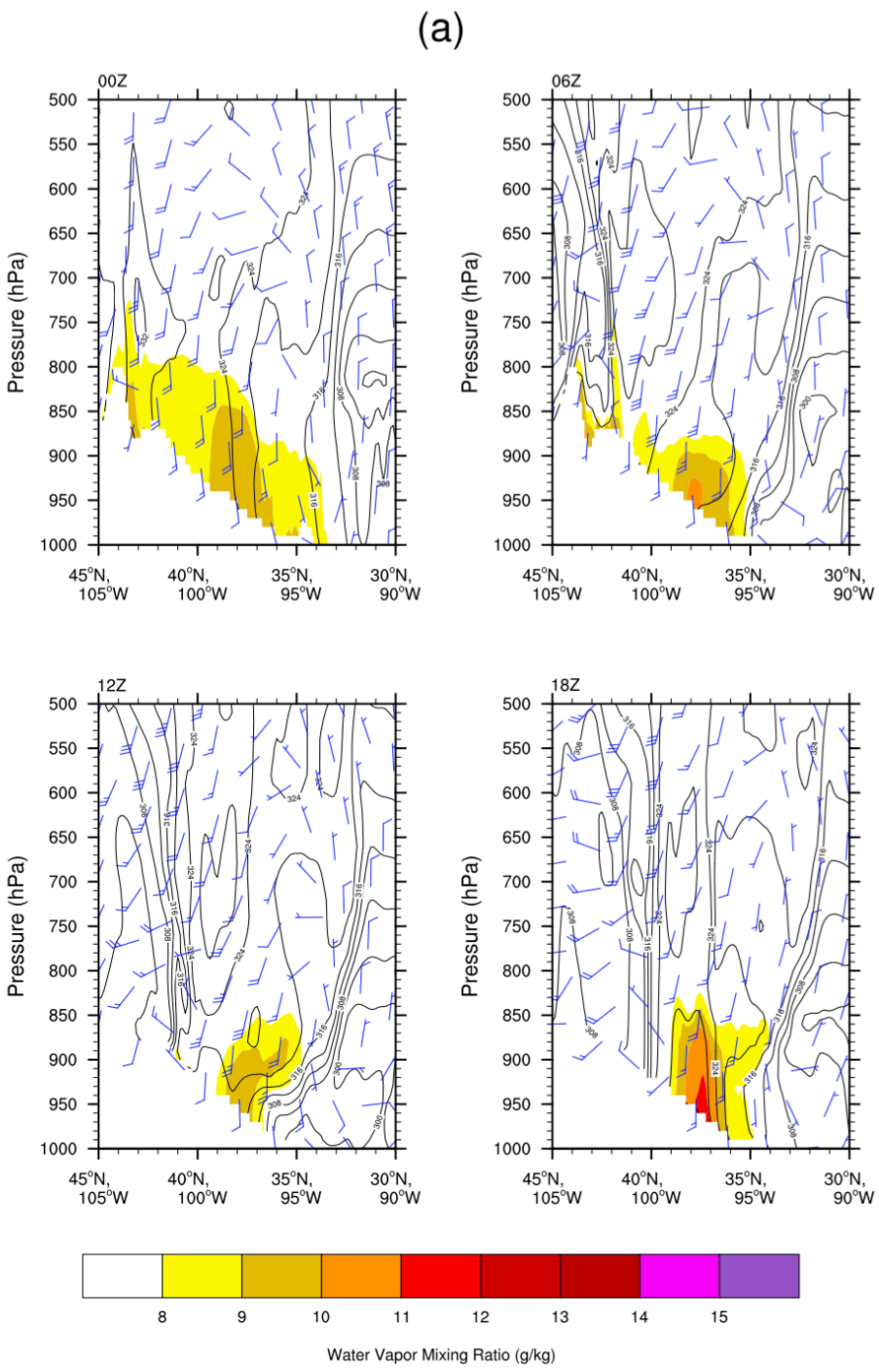
(a)
00Z
06Z
12Z
18Z
Pressure (hPa)
500
550
600
650
700
750
800
850
900
950
1000
45°N, 105°W
40°N, 100°W
35°N, 95°W
30°N, 90°W
8
9
10
11
12
13
14
15
Water Vapor Mixing Ratio (g/kg)

(b)

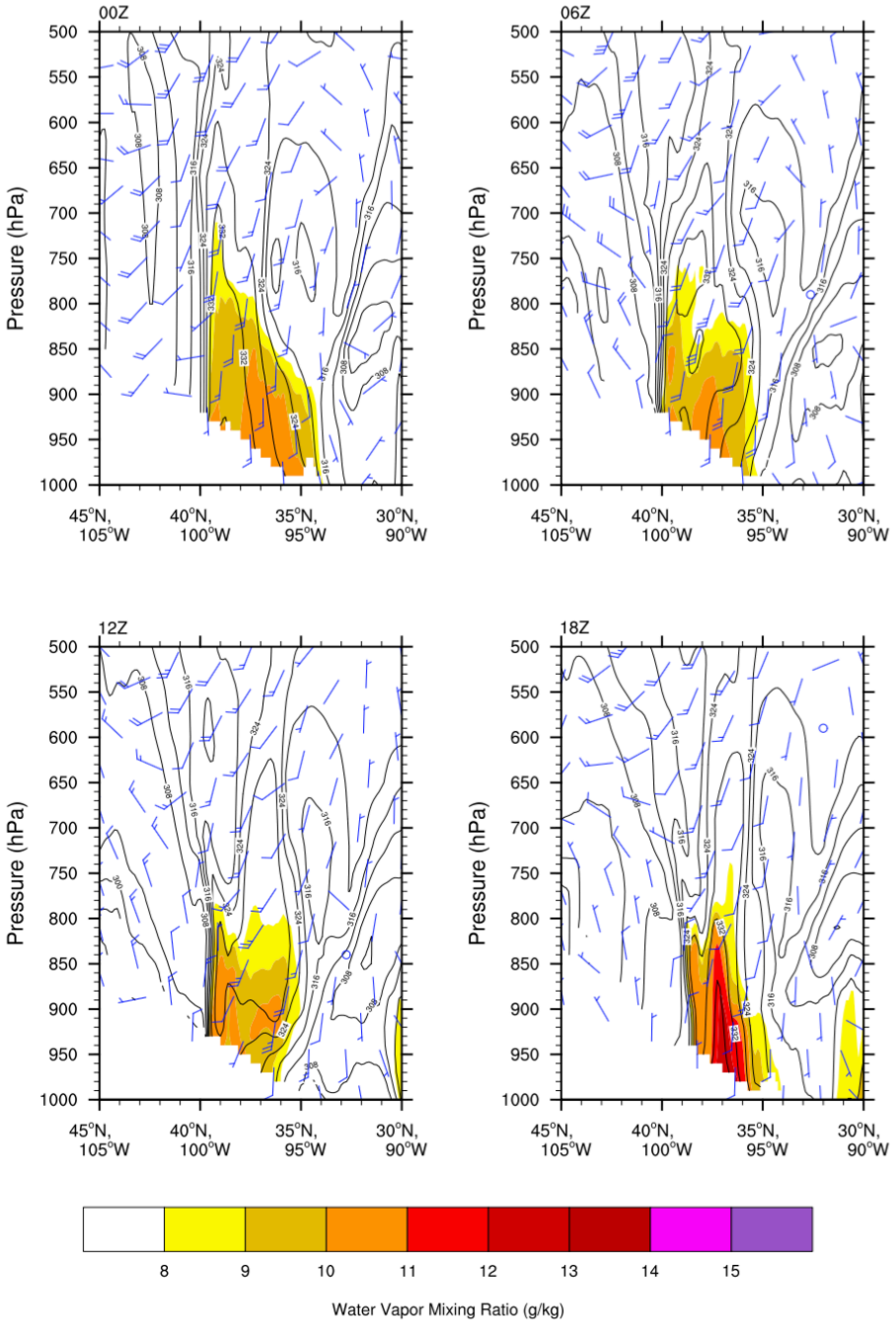
00Z
06Z
12Z
18Z
Pressure (hPa)
500
550
600
650
700
750
800
850
900
950
1000
45°N, 105°W
40°N, 100°W
35°N, 95°W
30°N, 90°W
8
9
10
11
12
13
14
15
Water Vapor Mixing Ratio (g/kg)

(c)

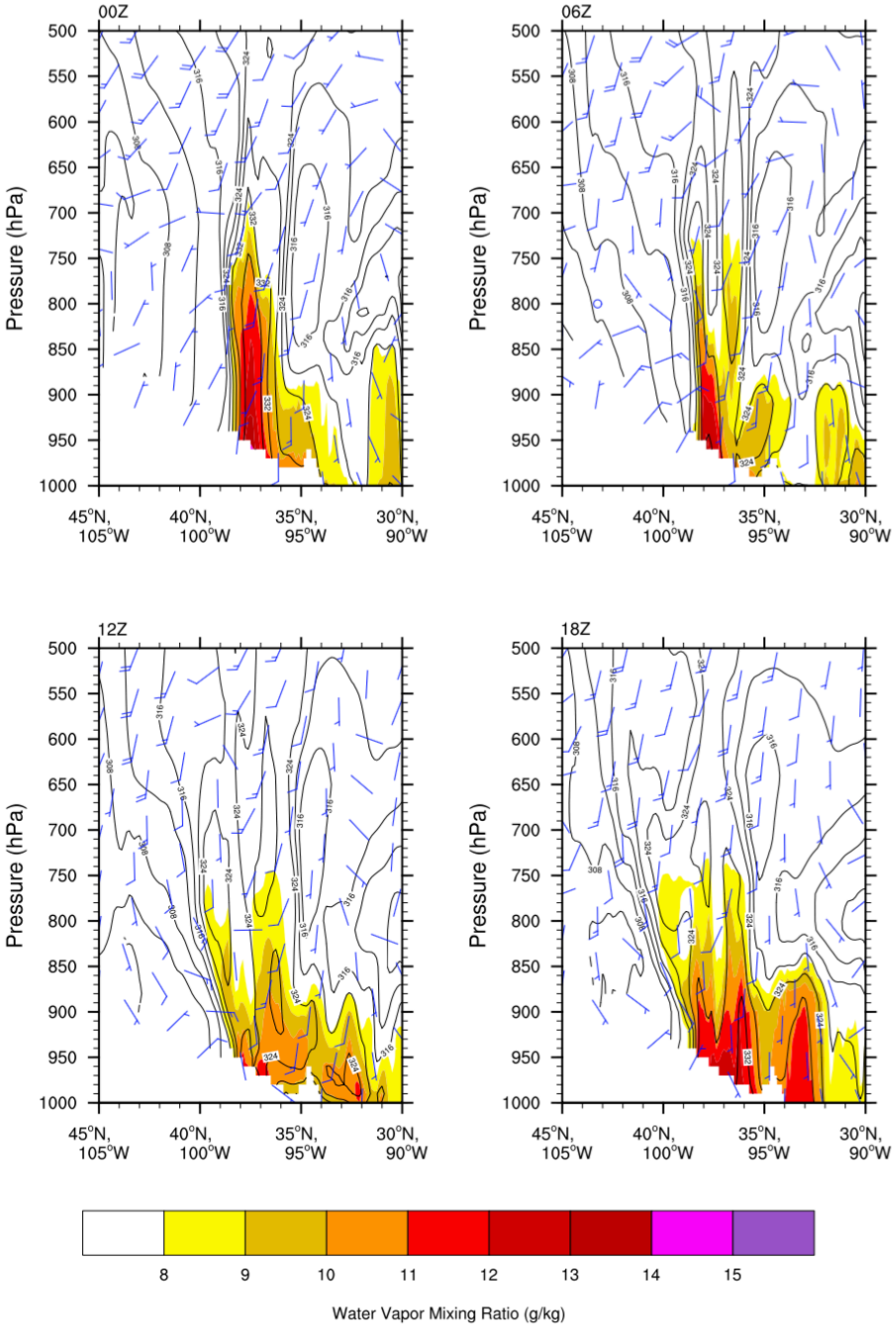
00Z
06Z
12Z
18Z
Pressure (hPa)
500
550
600
650
700
750
800
850
900
950
1000
45°N, 105°W
40°N, 100°W
35°N, 95°W
30°N, 90°W
8
9
10
11
12
13
14
15
Water Vapor Mixing Ratio (g/kg)

(d)

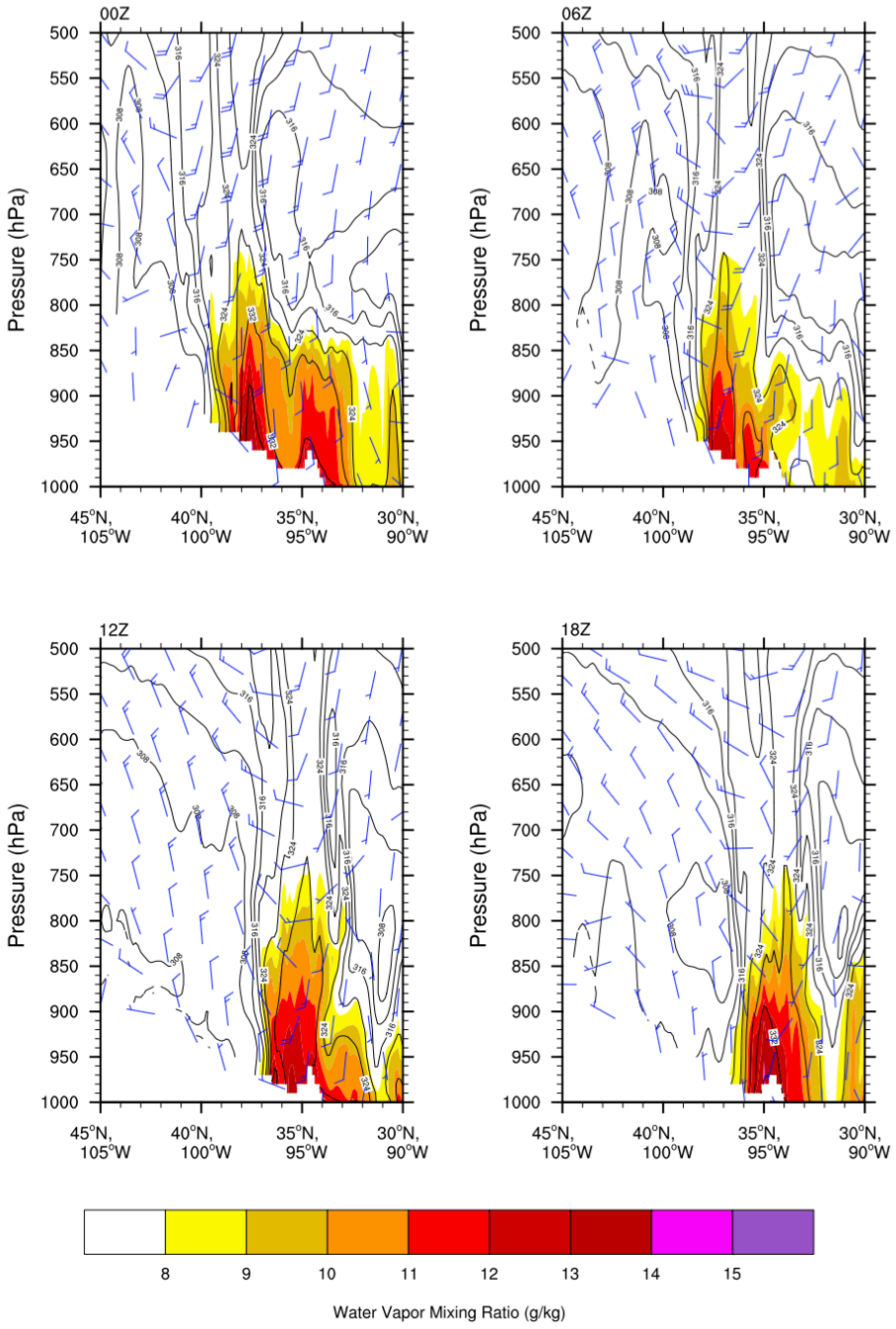
00Z
06Z
12Z
18Z
Pressure (hPa)
500
550
600
650
700
750
800
850
900
950
1000
45°N, 105°W
40°N, 100°W
35°N, 95°W
30°N, 90°W
8
9
10
11
12
13
14
15
Water Vapor Mixing Ratio (g/kg)

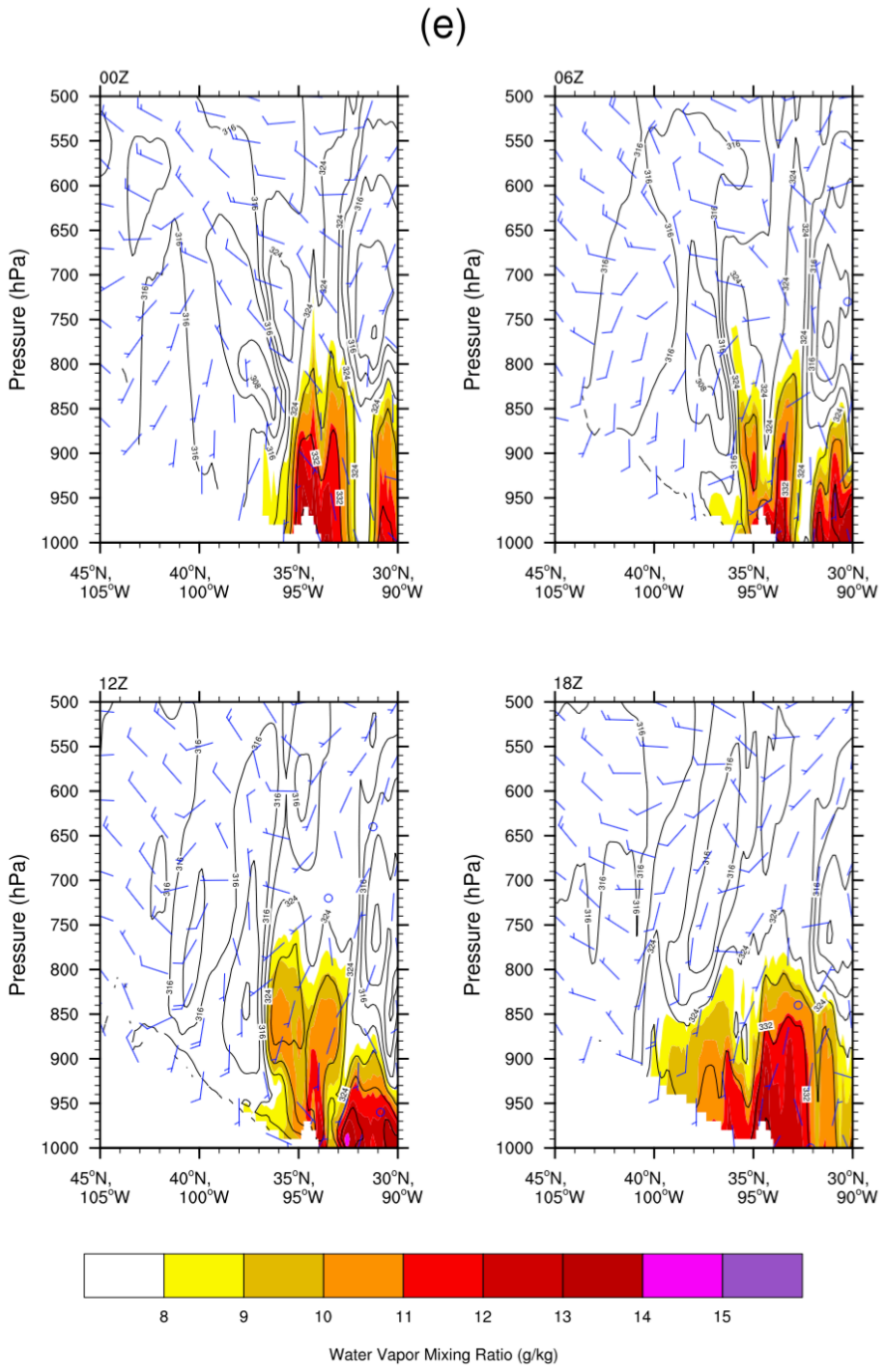

Figure 4.8 Vertical cross sections of winds (vector, unit: knots), equivalent potential temperature (black contour, unit: K) and water vapor mixing ratio (shaded with values greater or equal to 8g/kg, unit: g/kg) from May 22nd to 26th, 2002. (a) is May 22nd; (b) is May 23rd; (c) is May 24th; (d) is May 25th and (e) is May 26th.

To sum up, in the first case, the development of GPLLJ can be described by a two-layer mass adjustment model as the upper-level jet streak propagated eastward. Also, the upper- and lower-level jet divergence-convergence pattern provoked upward motion. After the GPLLJ was formed, warm, moist air was brought into the central U.S. area from the Gulf of Mexico, encountered dry air from northwest and formed a dryline in southeastern Kansas around midnight in May 24th. The moist environment and upward motion caused by the coupling of upper-lower level jet streaks produced precipitation. As the upper-level jet streak propagated eastward, the Wyoming-Colorado region was under less control of the upper-level divergence in May 25th. The weakened GPLLJ was then located in the eastern Oklahoma-Texas area, and subsequently retreated southward. However, the moisture was still in the Kansas area and maintained the precipitation there during May 25th. On May 26th, the moisture effects of the GPLLJ and dynamic mechanism of coupling of upper and lower jet streak dissipated. There were no obvious GPLLJ and precipitation activities. In this case, the GPLLJ not only played the role of moisture transportation, but also interactive with synoptic scale systems to create rising motion, which triggered precipitation eventually.

Figure 4.9 shows the precipitation and the GPLLJ activity indicators from July 17th to July 19th. The main precipitation events we focused on analyzing was July 18th and July 19th. In July 17th (Figure 4.9a), precipitation occurred in the northern Texas around 06Z. In July 18th (Figure 4.9b), precipitation occurred in the boundary area of Kansas-Oklahoma and Missouri-Arkansas, about 35°-40°N, 97°-92°W. In July 19th (Figure 4.9c), the precipitation moved eastward, around the area of 35°-36°N, 96°-94°W. In the second case, the diurnal cycle of precipitation was a little different compared to the first case. In the first

case, the nocturnal peak of precipitation was dominant. However, in the second case, the precipitation didn't have much diurnal variability, especially on July 18th.

In the second case, the GPLLJ was relatively weak (can be seen in Figure 4.5). In Figure 4.9, for the consideration of showing the wind direction and circulation more clearly, wind barb was plotted with a certain length and that led to winds at some grid point not being plotted. For that reason, wind barb may not be able to show the actual wind speed in the interested area. From Figure 4.5b, wind speed at 925 hPa was maximum and can represent the intensity of the GPLLJ. In July 17th (Figure 4.9a), the GPLLJ area was broad (from Texas to North Dakota) and the intensity was relatively strong (maximum wind speed around 18 m/s). From July 18th (Figure 4.9b), the high low-level wind speed area shrunk down considerably, focused in the eastern area of Texas and Oklahoma and western Arkansas, about 30°-37°N, 100°-93°W. The diurnal cycle of the GPLLJ wasn't that obvious compared to the first case either. In July 19th (Figure 4.9c), the intensity of the GPLLJ decreased further, staying just around the area of eastern Texas and Oklahoma, about 30°-35°N, 100°-95°W. Also, judging by the wind speed, a clear wind speed boundary showed up in the central Texas in 06Z and 12Z.

(a)

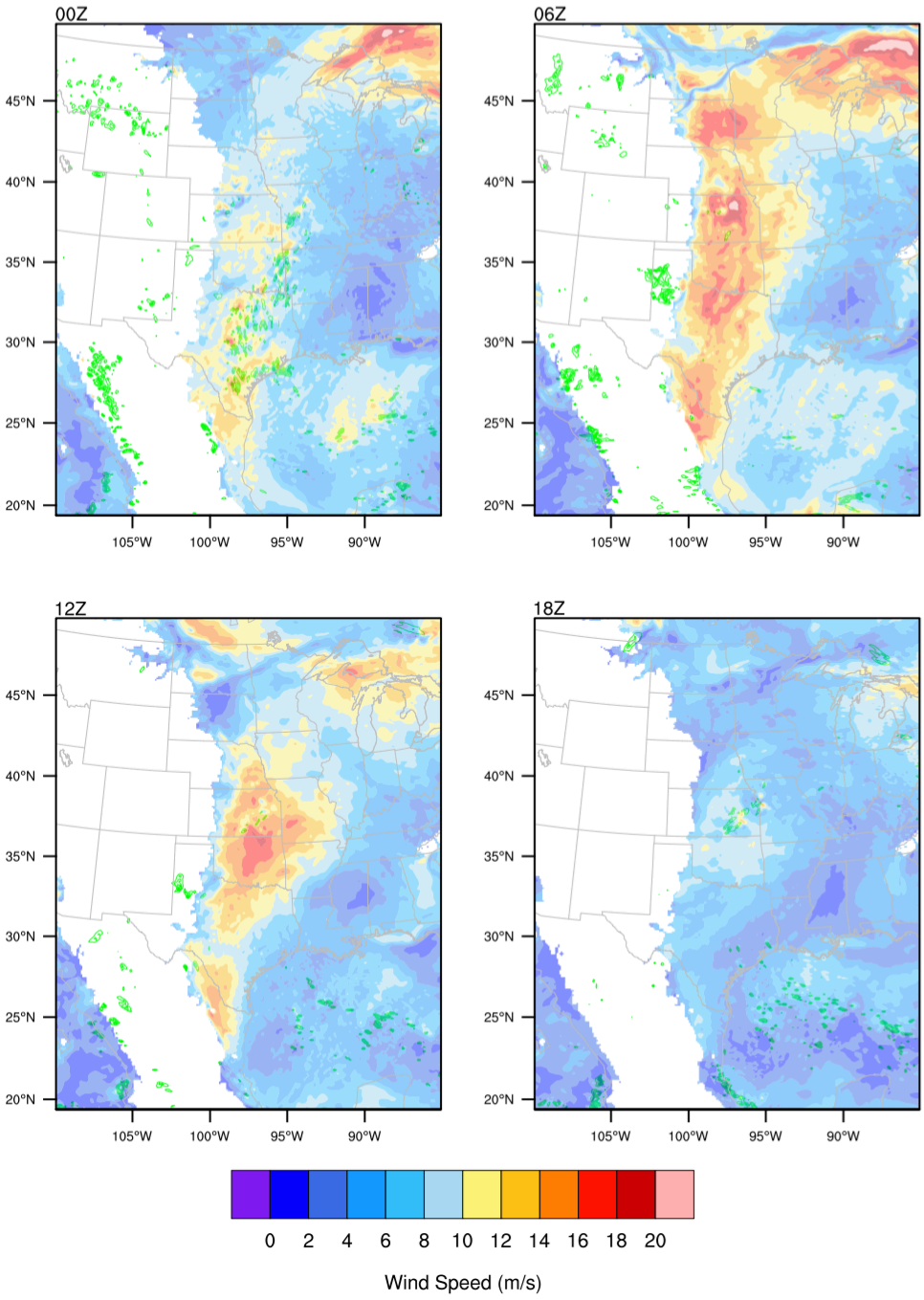
00Z
06Z
12Z
18Z
45°N
40°N
35°N
30°N
25°N
20°N
105°W
100°W
95°W
90°W
0 2 4 6 8 10 12 14 16 18 20
Wind Speed (m/s)

(b)

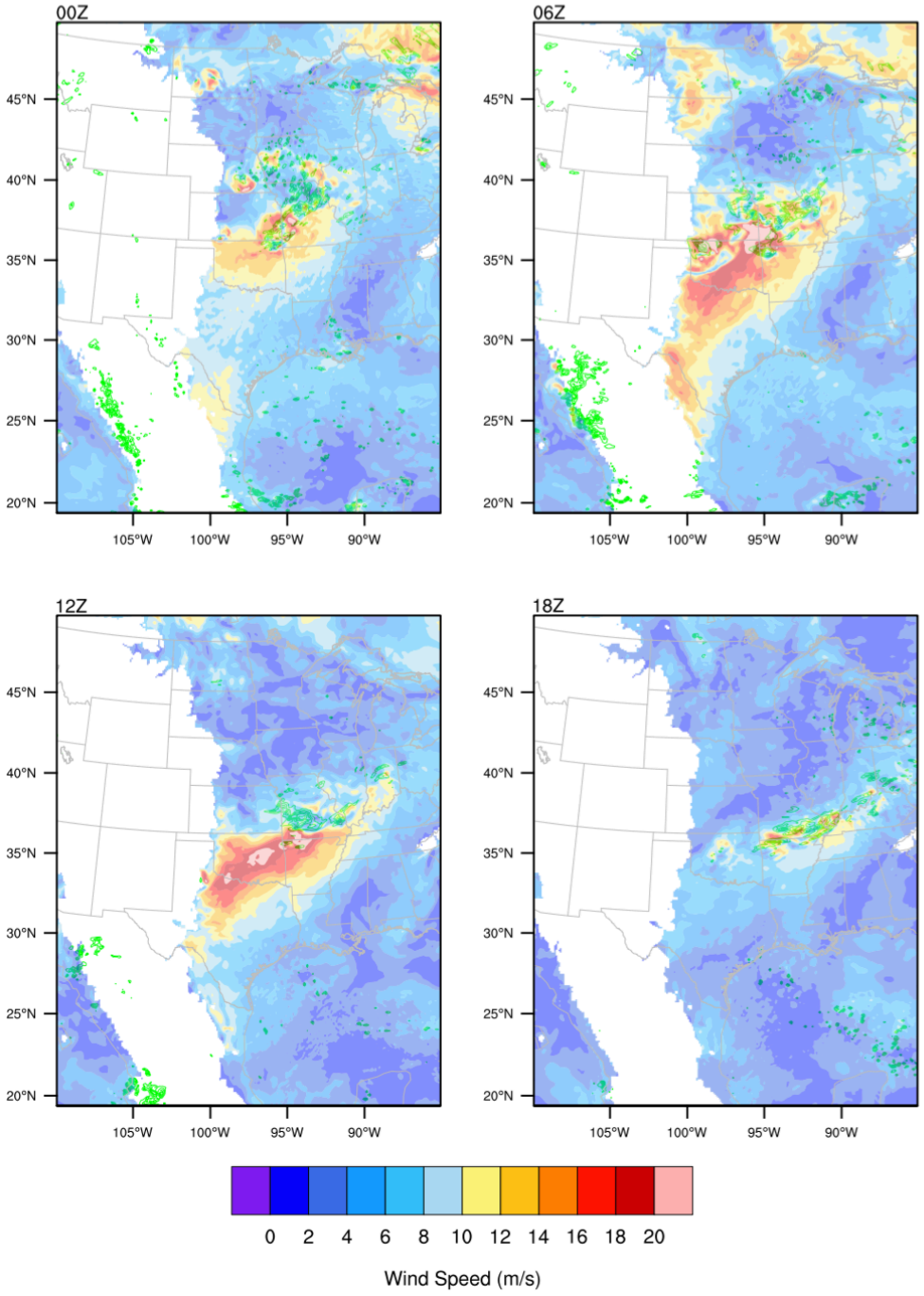
00Z
06Z
12Z
18Z
45°N
40°N
35°N
30°N
25°N
20°N
105°W
100°W
95°W
90°W
0 2 4 6 8 10 12 14 16 18 20
Wind Speed (m/s)

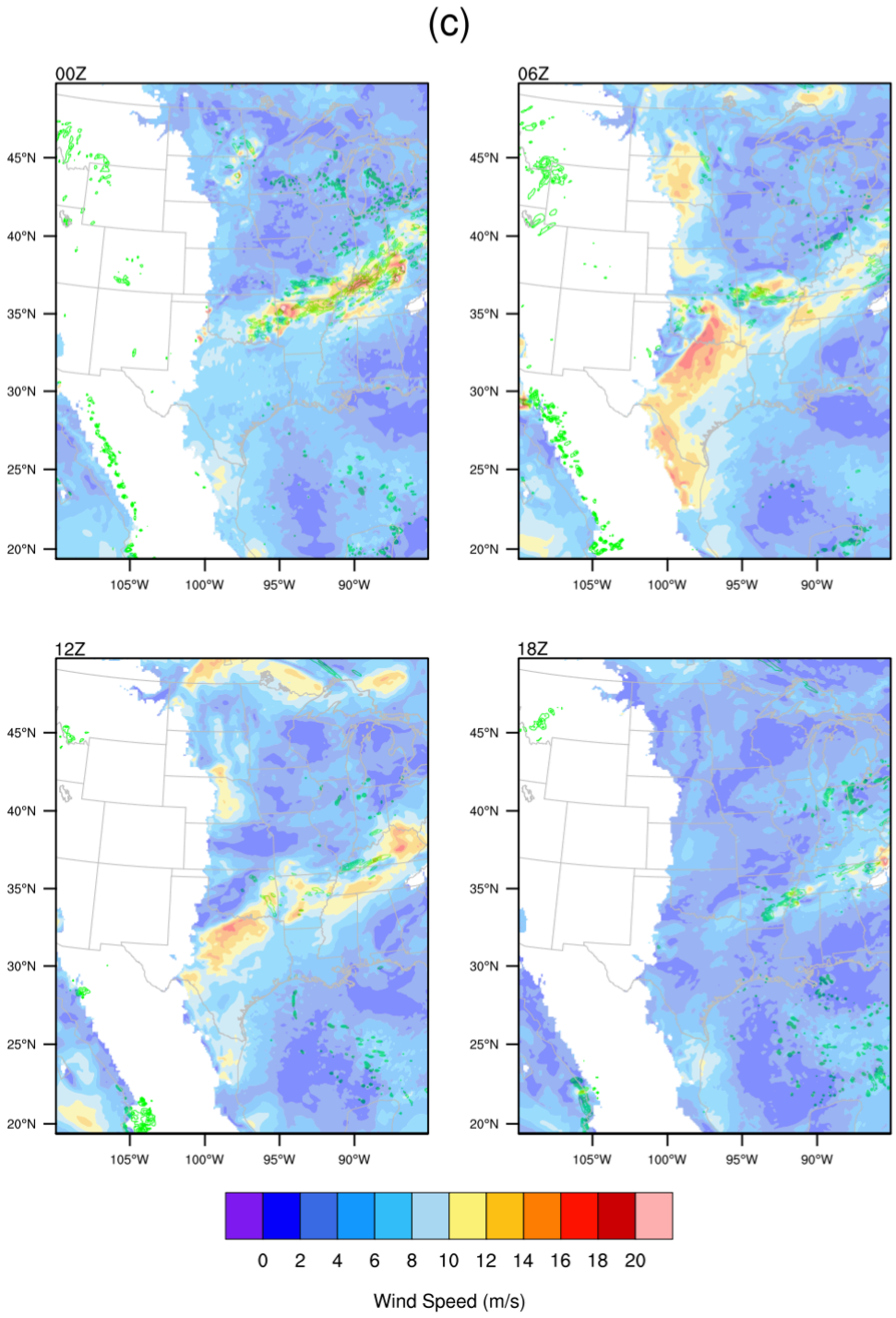

Figure 4.9 Wind speed at 925 hPa (shaded, unit: m/s) and precipitation (green contour, contoured from 0 mm/6hours to 60 mm/6hours by 10 mm/6hours, unit: mm/6hours) from July 17th to 19th, 2002. (a) is July 17th; (b) is July 18th and (c) is July 19th.

Figure 4.10 shows the dew point at 2 meters, 6 hourly isallobars, precipitation and 925 hPa wind direction. According to the dew point at 2 meters and 6 hourly isallobars, it appears that in the precipitation area, a front passed through on July 18th (Figure 4.10b). Before the passage of the front, even with broad GPLLJ activity, there was no precipitation at the north nose of the GPLLJ. When the front passed in July 18th, precipitation started to form along the northern boundary of Kansas and Missouri. To the south of the precipitation, the dew point was higher, while in the northern part of precipitation there was lower dew point at 2 meters. Combined with the tighter isallobars in the precipitation area and the shear of low-level wind, the precipitation seems related to a weak warm frontal system. By July 19th (Figure 4.10c), after the passage of the front, precipitation started to dissipate.

Figure 4.11 shows the vertical cross sections of winds, equivalent potential temperature and water mixing ratio perpendicular to the precipitation area. According to Figure 4.11, the equivalent potential temperature and water vapor mixing ratio were consistently higher than in the first case for an overall warmer atmosphere can hold more water. The vertical gradient of equivalent potential temperature means the atmosphere was more unstable in the second case than in the first case. It is clear that in July 18th (Figure 4.11b), especially from 06Z, the moisture was lifted up around the precipitation area compared to July 17th (Figure 4.11a). From Figure 4.11, we can see in the southern part of precipitation (represent by 35°N, 90°W on Figure 4.11), there was more moisture than in the northern part (represented by 40°N, 95°W on Figure 4.11).

(a)

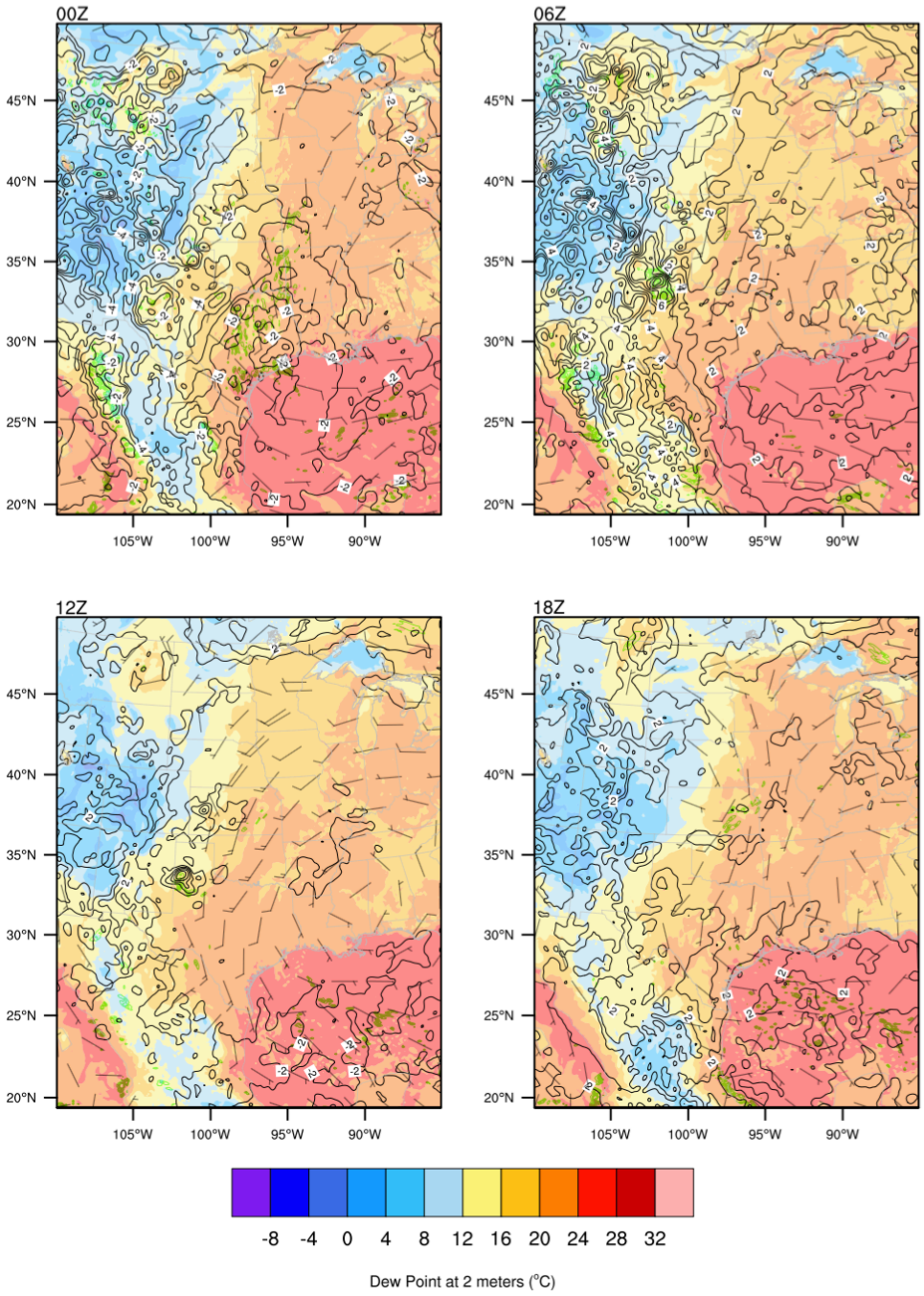
00Z
06Z
12Z
18Z
45°N
40°N
35°N
30°N
25°N
20°N
105°W
100°W
95°W
90°W
-8 -4 0 4 8 12 16 20 24 28 32
Dew Point at 2 meters (°C)

(b)

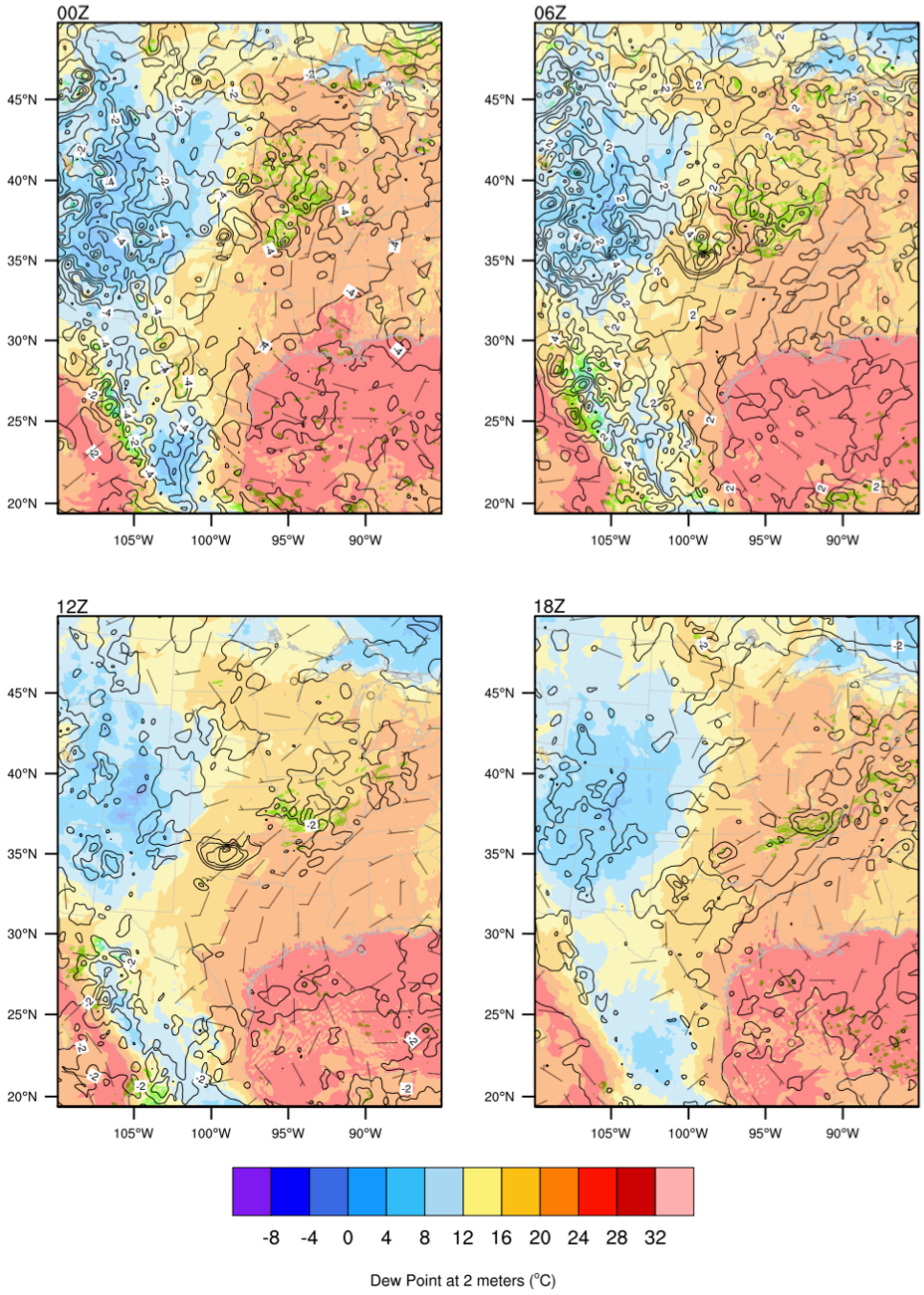
00Z
06Z
12Z
18Z
45°N
40°N
35°N
30°N
25°N
20°N
105°W
100°W
95°W
90°W
-8 -4 0 4 8 12 16 20 24 28 32
Dew Point at 2 meters (°C)

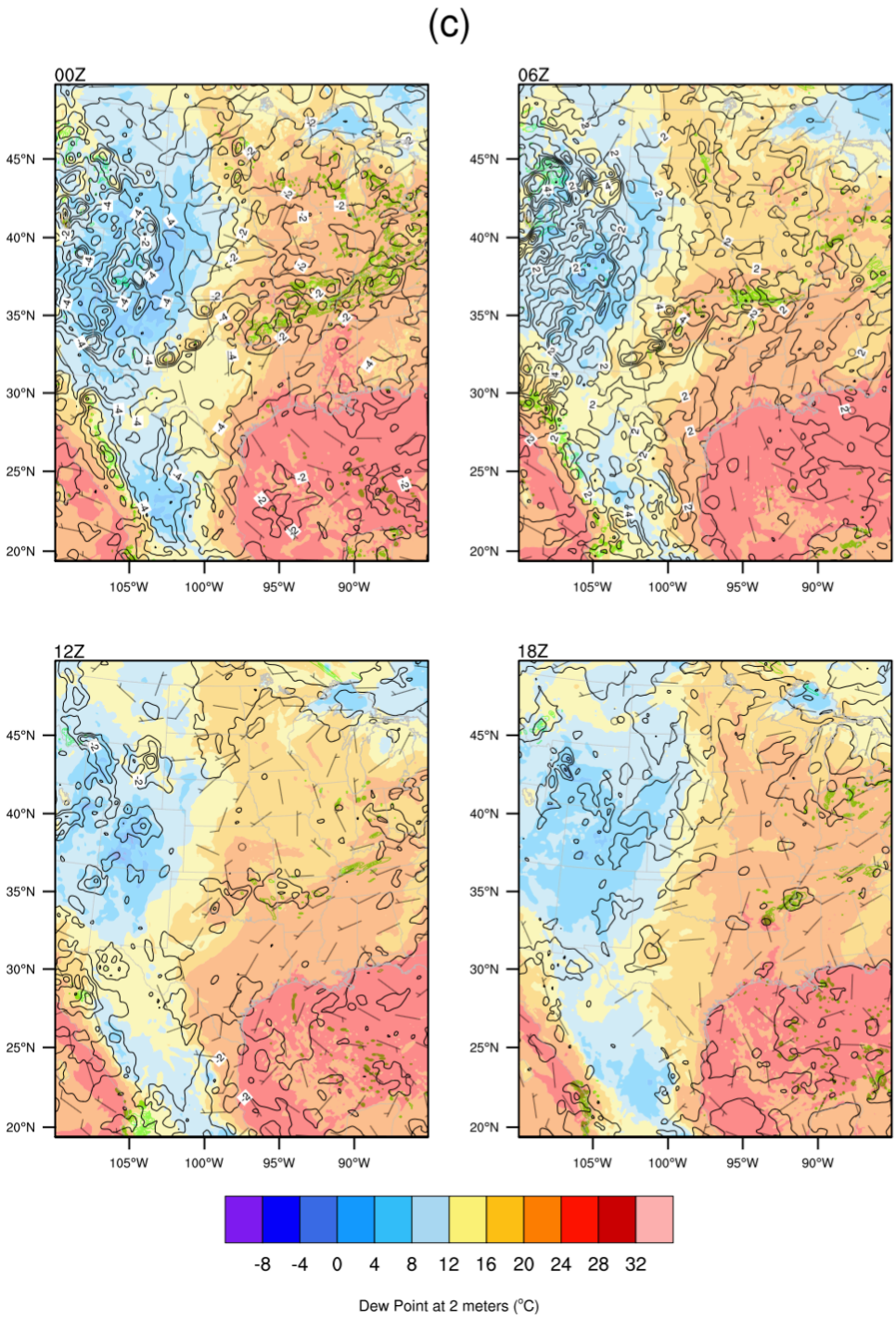

Figure 4.10 Dew point at 2 meters (shaded, unit: °C), 6 hourly isallobars (black contour, unit: hPa/6hours), precipitation (green contour, contoured from 0 mm/6hours to 60 mm/6hours by 10 mm/6hours, unit: mm/6hours) and winds at 925 hPa (vector, unit: knots) from July 17th to19th, 2002. (a) is July 17th; (b) is July 18th and (c) is July 19th.

(a)

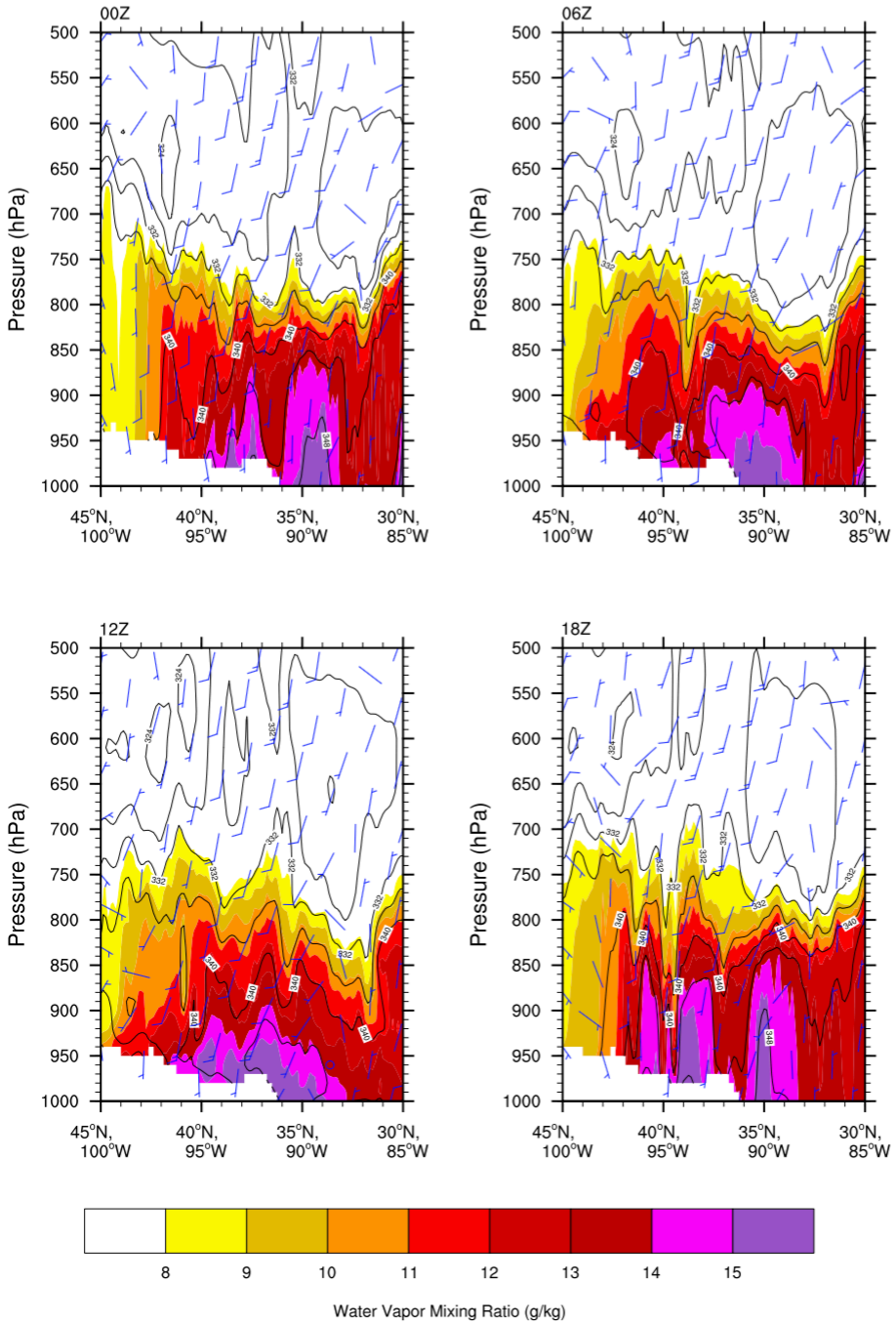
00Z
06Z
12Z
18Z
Pressure (hPa)
500
550
600
650
700
750
800
850
900
950
1000
45°N, 100°W
40°N, 95°W
35°N, 90°W
30°N, 85°W
8
9
10
11
12
13
14
15
Water Vapor Mixing Ratio (g/kg)

(b)

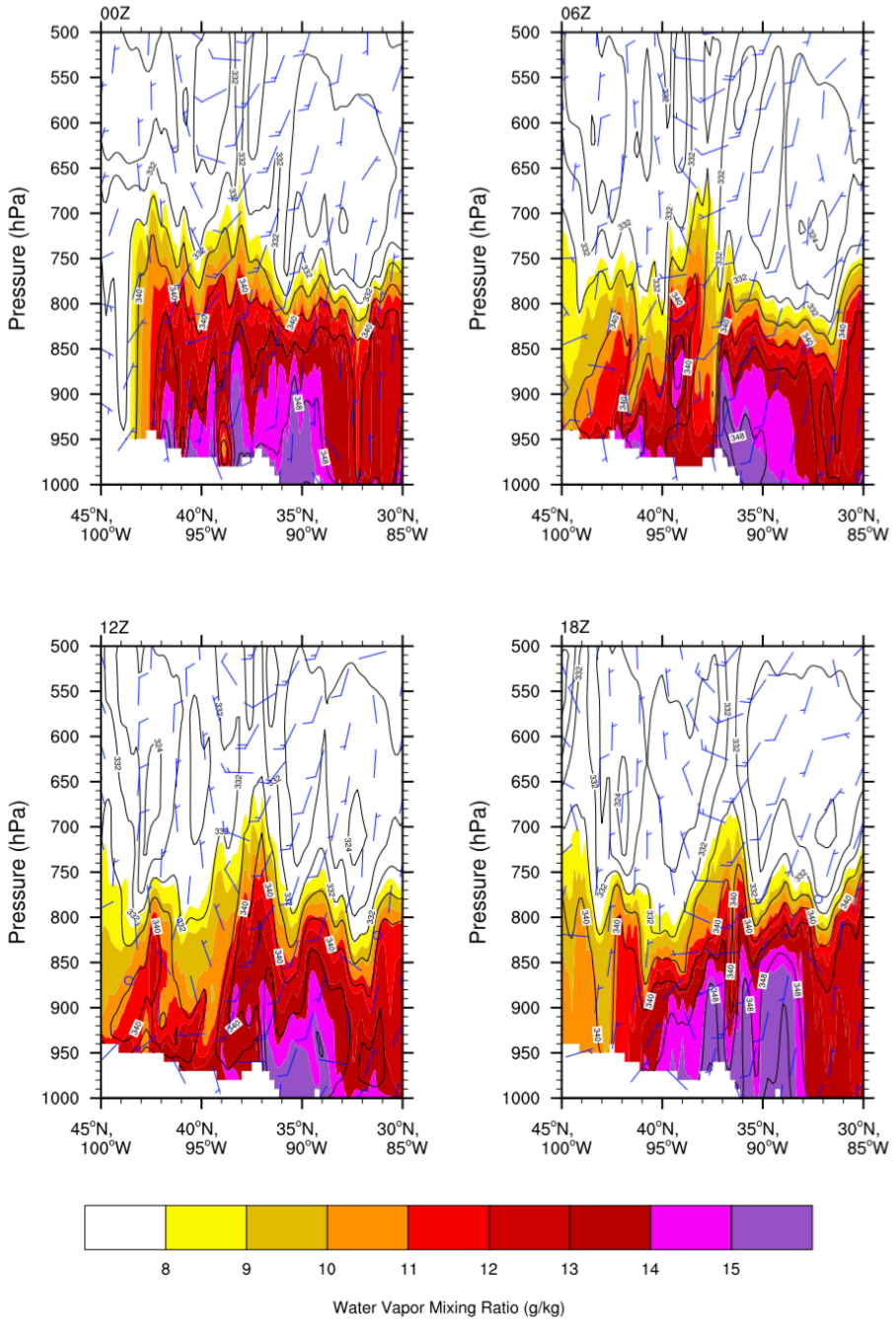
00Z
06Z
12Z
18Z
Pressure (hPa)
500
550
600
650
700
750
800
850
900
950
1000
45°N, 100°W
40°N, 95°W
35°N, 90°W
30°N, 85°W
8
9
10
11
12
13
14
15
Water Vapor Mixing Ratio (g/kg)

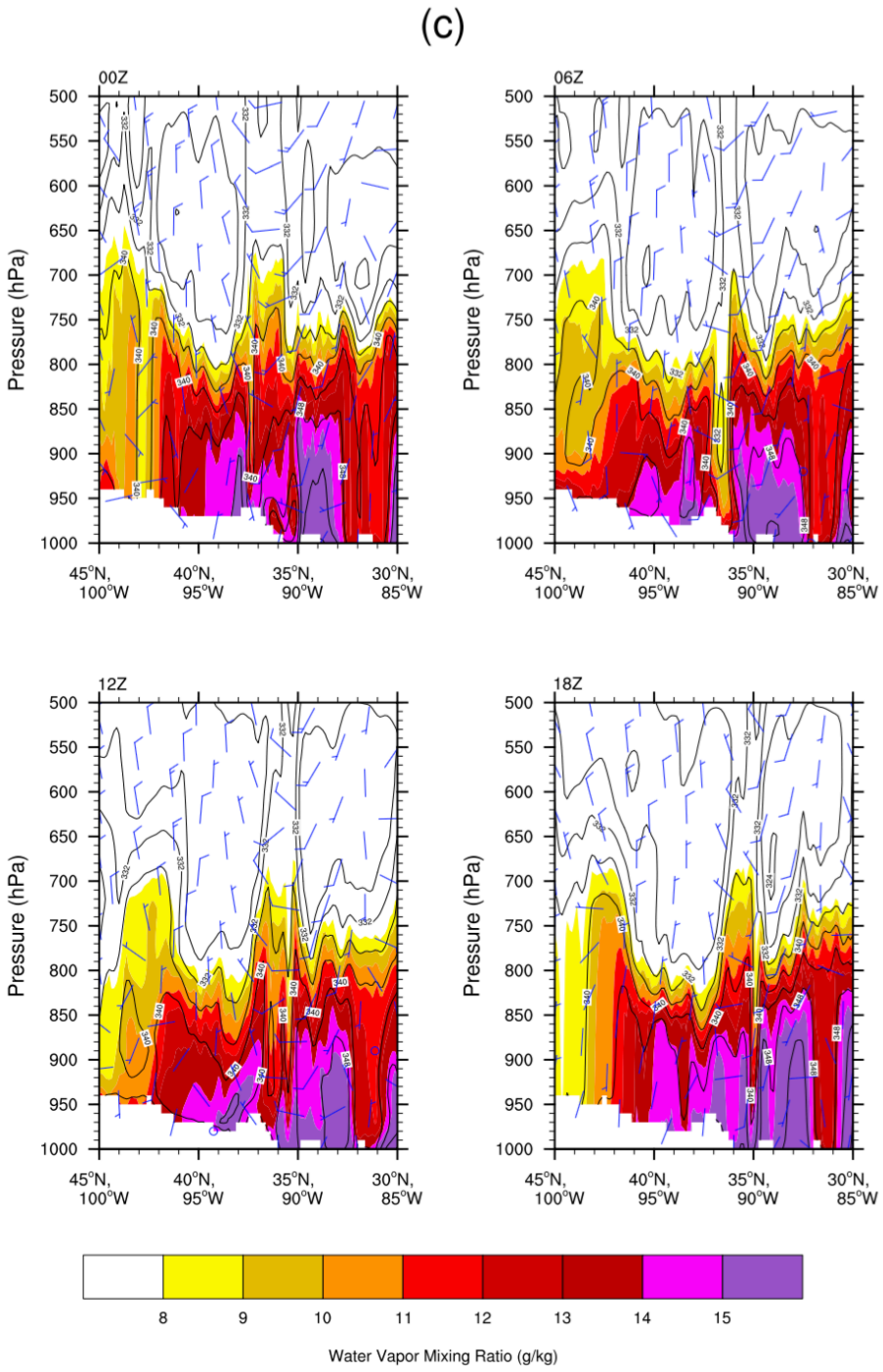

Figure 4.11 Vertical cross sections of winds (vector, unit: knots), equivalent potential temperature (black contour, unit: K) and water vapor mixing ratio (shaded with values greater or equal to 8g/kg, unit: g/kg) from July 17th to 19th, 2002. (a) is July 17th; (b) is July 18th and (c) is July 19th.

We can see that on July 17th, although there was GPLLJ activity, there was no obvious precipitation at the nose of the GPLLJ. In July 18th and 19th, the GPLLJ area decreased but precipitation started to appear. Combined with the frontal system information from Figure 4.10, we can see the precipitation in the second case was closely related to the activity of the frontal system. In July 17th, there was little effect from frontal system. Even with the GPLLJ activity, there was no lifting mechanism for precipitation formation. In July 18th and 19th, a frontal system formed. The surface front was in the area of 35°-40°N, 97°-92°W and moved eastward. When the GPLLJ transported moisture from the Gulf of Mexico, the moisture from the south was forced to rise because of the frontal boundary, then the rising motion encountered the relatively unstable atmosphere, causing precipitation along the boundary. However, the moisture cannot reach northward for it was lifted up. For that reason, there were more moisture in the southern part of the precipitation, as we can see in Figure 4.11b-c. In this case, the main effect of the GPLLJ was transportation of moisture, the dynamic trigger was based on the frontal system. Without the front, even though there was GPLLJ event, there likely would have been no precipitation.

By comparing these two cases, we can conclude in the “wet period”, when the synoptic scale system was more active, the GPLLJ not only transported moisture, but also interacted with synoptic system to trigger the precipitation. However, in the “dry period”, the main effect of the GPLLJ was moisture transportation. The development of precipitation was closely related to a mesoscale system such as the passage of frontal system.

Chapter 5

Summary and Future Work

5.1 Summary

This study focused on obtaining a better understanding of different mechanisms of how the Great Plains Low-level Jet (GPLLJ) can promote warm season precipitation over the central U.S. To achieve this goal, the Weather Research and Forecasting (WRF) regional model was used to simulate May 1st to August 31st, 2002.

Year 2002 was selected by going through 35 years (from 1979 to 2013) of NARR data. We used NARR meridional and zonal winds as well as precipitation data to compare and select a year with a relatively "wet period" and a relatively "dry period". In 2002, there were more precipitation events in May and June, referred as the "wet period"; in July and August, the precipitation events decreased, referred as the "dry period".

We next used WRF driven by 3 hourly NARR data to simulate the warm season of year 2002. In the model set up, we used a domain that covers all of continental U.S. and the Gulf of Mexico with a high spatial resolution of 10 kilometers. To better simulate the precipitation activities, several tests of parameterization were conducted. We focused on the test of cumulus parameterization and found in this case, using the Grell-Freitas scheme worked better for precipitation simulation. After the model experiments were done, we used NARR data to validate WRF winds and precipitation results. Further validation of precipitation was done using CPC observed rainfall data. It turned out WRF simulation results were relatively accurate and can be used for further analysis.

We compared the GPLLJ and synoptic scale systems activities as well as moisture advection in the "wet period" and the "dry period". From the seasonal variability of the

GPLLJ, it seems like the GPLLJ was generally stronger and more active in the "wet period" than in the "dry period". The GPLLJ core moved northward from the "wet period" to the "dry period". The precipitation usually occurred at the nose of the GPLLJ in the "wet period" when in the "dry period", there was less obvious precipitation mechanisms. The filtered 2-6 days' scale synoptic systems showed that the synoptic systems were more active in May and June. From the aspect of moisture advection, the strength and trajectory changes were similar to the GPLLJ activities, indicating the GPLLJ events were closely related in terms of the transportation of moisture.

The comparisons between two periods provided differences of the background atmospheric state between the "wet period" and "dry period". For the purpose of this study, individual cases would be better for dynamic analysis. We selected two precipitation cases with GPLLJ event. One case was chosen from the "wet period" and the other one was chosen from the "dry period".

In the case from the "wet period", the GPLLJ might be resulted from the propagation of the upper-level jet streak. The divergence in the cyclonic side of the upper-level jet streak exit region was compensated by the convergence in the lower-level, which increased the isallobaric wind in the lower-level (Uccellini and Johnson 1979). The low-level isallobaric wind contributed significantly to the development of the GPLLJ (Uccellini and Johnson 1979). The coupling of the upper-level divergence and lower-level convergence created rising motion. Combined with moisture from the Gulf of Mexico transported by the GPLLJ, precipitation started to develop. In this case, the GPLLJ not only transported moisture from the south but also provided a dynamic trigger by coupling with upper-level jet streak.

For the second case, the formation of precipitation was more related to mesoscale systems such as frontal system. The main role of the GPLLJ was moisture transport. With a frontal system passing through, the moisture transported by the GPLLJ encountered the front and was forced to rise. Combined with the unstable atmosphere, precipitation started to develop.

From the case studies, we can see when synoptic scale systems were more active, the GPLLJ had two main effects: interact with synoptic systems to provide dynamic trigger and transportation of moisture. With the absence of synoptic systems, the main effect of the GPLLJ was transporting moisture.

5.2 Future Work

While this work compared different roles of the GPLLJ played in producing warm season precipitation in the central U.S., it can be strengthened by studying more cases. Because of limited resources and time, only two cases from one year were studied in this work. With only two cases, it can be argued that the different mechanisms of how the GPLLJ promotes precipitation might hold just for those cases. The universality of those two dynamic processes and other possible processes should be tested or modified in future work.

Several years can be selected to better understanding the climatology of the GPLLJ, precipitation and possible influencing factors such as synoptic forcing. At least two or three more cases should be selected and compared. The comparison between strong precipitation with strong GPLLJ, weak precipitation with strong GPLLJ and strong precipitation with weak GPLLJ and weak precipitation with weak GPLLJ can be done to show the importance

of dynamic processes mentioned in this study. Neutral GPLLJ can be used as a control case as well.

The accuracy of model results can also be improved by testing of even higher resolution and possible better combinations of parameterization. Although in Chapter 3, it was mentioned the model results with 4 kilometers resolution was similar to the ones with 10 kilometers resolution, higher resolution might make a difference with a different year. Also, in this study's model set up, we focused on the testing of the cumulus parameterization. In the future, the combination of land model, cumulus and other possible influencing parameterization can be tested and used for different year and case selections.

References

Arritt, R. W., T. D. Rink, M. Segal, D. P. Todey, C. A. Clark, M. J. Mitchell, and K. M. Labas, 1997: The great plains low-level jet during the warm season of 1993. *Mon Weather Rev*, **125,** 2176-2192.

Augustine, J. A., and K. W. Howard, 1991: Mesoscale convective complexes over the United States during 1986 and 1987. *Mon Weather Rev*, **119,** 1575-1589.

Bonner, W. D., 1968: Climatology of Low Level Jet. *Mon Weather Rev*, **96,** 833-&.

Carbone, R. E., J. D. Tuttle, D. A. Ahijevych, and S. B. Trier, 2002: Inferences of predictability associated with warm season precipitation episodes. *J Atmos Sci*, **59,** 2033-2056.

Chen, M., W. Shi, P. Xie, V. Silva, V. E. Kousky, R. Wayne Higgins, and J. E. Janowiak, 2008: Assessing objective techniques for gauge-based analyses of global daily precipitation. *Journal of Geophysical Research: Atmospheres (1984–2012)*, **113**.

Chen, T. C., and J. A. Kpaeyeh, 1993: The Synoptic-Scale Environment Associated with the Low-Level Jet of the Great-Plains. *Mon Weather Rev*, **121,** 416-420.

Cook, K. H., E. K. Vizy, Z. S. Launer, and C. M. Patricola, 2008: Springtime Intensification of the Great Plains Low-Level Jet and Midwest Precipitation in GCM Simulations of the Twenty-First Century. *J Climate*, **21,** 6321-6340.

Ghan, S. J., X. D. Bian, and L. Corsetti, 1996: Simulation of the great plains low-level jet and associated clouds by general circulation models. *Mon Weather Rev*, **124,** 1388-1408.

Grell, G. A., and S. R. Freitas, 2013: A scale and aerosol aware stochastic convective parameterization for weather and air quality modeling. *Atmos. Chem. Phys. Discuss*,

13, 845-823.

Helfand, H. M., and S. D. Schubert, 1995: Climatology of the Simulated Great-Plains Low-Level Jet and Its Contribution to the Continental Moisture Budget of the United-States. *J Climate*, **8,** 784-806.

Higgins, R. W., Y. Yao, E. S. Yarosh, J. E. Janowiak, and K. C. Mo, 1997: Influence of the Great Plains low-level jet on summertime precipitation and moisture transport over the central United States. *J Climate*, **10,** 481-507.

Holton, J. R., 1967: Diurnal Boundary Layer Wind Oscillation above Sloping Terrain. *Tellus*, **19,** 199-&.

Hu, Q., and S. Feng, 2001: Climatic role of the southerly flow from the Gulf of Mexico in interannual variations in summer rainfall in the central United States. *J Climate*, **14,** 3156-3170.

Jiang, X. N., N. C. Lau, and S. A. Klein, 2006: Role of eastward propagating convection systems in the diurnal cycle and seasonal mean of summertime rainfall over the U.S. Great Plains. *Geophys Res Lett*, **33**.

Kain, J. S., 2004: The Kain-Fritsch convective parameterization: an update. *Journal of Applied Meteorology*, **43,** 170-181.

Lee, M.-I., I. Choi, W.-K. Tao, S. D. Schubert, and I.-S. Kang, 2010: Mechanisms of diurnal precipitation over the US Great Plains: a cloud resolving model perspective. *Climate dynamics*, **34,** 419-437.

Lee, M. I., S. D. Schubert, M. J. Suarez, J. K. E. Schemm, H. L. Pan, J. Han, and S. H. Yoo, 2008: Role of convection triggers in the simulation of the diurnal cycle of precipitation over the United States Great Plains in a general circulation model.

Journal of Geophysical Research: Atmospheres (1984–2012), **113**.

Lee, M. I., and Coauthors, 2007: An analysis of the warm-season diurnal cycle over the continental united states and northern Mexico in general circulation models. *J Hydrometeorol*, **8,** 344-366.

Liang, X. Z., L. Li, A. Dai, and K. E. Kunkel, 2004: Regional climate model simulation of summer precipitation diurnal cycle over the United States. *Geophys Res Lett*, **31**.

McCorcle, M. D., 1988: Simulation of Surface-Moisture Effects on the Great Plains Low-Level Jet. *Mon Weather Rev*, **116,** 1705-1720.

Mesinger, F., and Coauthors, 2006: North American regional reanalysis. *Bulletin of the American Meteorological Society*, **87,** 343-360.

Mitchell, M. J., R. W. Arritt, and K. Labas, 1995: A Climatology of the Warm-Season Great-Plains Low-Level Jet Using Wind Profiler Observations. *Weather Forecast*, **10,** 576-591.

Pitchford, K. L., and J. London, 1962: The low-level jet as related to nocturnal thunderstorms over midwest United States. *Journal of Applied Meteorology*, **1,** 43-47.

Pu, B., and R. E. Dickinson, 2014: Diurnal Spatial Variability of Great Plains Summer Precipitation Related to the Dynamics of the Low-Level Jet. *J Atmos Sci*, **71,** 1807-1817.

Ruiz-Barradas, A., and S. Nigam, 2006: Great plains hydroclimate variability: The view from North American regional reanalysis. *J Climate*, **19,** 3004-3010.

Skamarock, W., J. Klemp, J. Dudhia, D. Gill, and D. Barker, 2005: Coauthors, 2008: A description of the Advanced Research WRF version 3. NCAR Tech.

Ting, M. F., and H. L. Wang, 2006: The role of the north American topography on the

maintenance of the great plains summer low-level jet. *J Atmos Sci*, **63,** 1056-1068.

Tollerud, E. I., and Coauthors, 2008: Mesoscale Moisture Transport by the Low-Level Jet during the IHOP Field Experiment. *Mon Weather Rev*, **136,** 3781-3795.

Uccellini, L. W., 1980: On the role of upper tropospheric jet streaks and leeside cyclogenesis in the development of low-level jets in the Great Plains. *Mon Weather Rev*, **108,** 1689-1696.

Uccellini, L. W., and D. R. Johnson, 1979: Coupling of Upper and Lower Tropospheric Jet Streaks and Implications for the Development of Severe Convective Storms. *Mon Weather Rev*, **107,** 682-703.

Wallace, J. M., 1975: Diurnal-Variations in Precipitation and Thunderstorm Frequency over Conterminous United-States. *Mon Weather Rev*, **103,** 406-419.

Wang, S. Y., and T. C. Chen, 2009: The Late-Spring Maximum of Rainfall over the US Central Plains and the Role of the Low-Level Jet. *J Climate*, **22,** 4696-4709.

Weaver, S. J., and S. Nigam, 2008: Variability of the great plains low-level jet: Large-scale circulation context and hydroclimate impacts. *J Climate*, **21,** 1532-1551.

Wu, Y. H., and S. Raman, 1998: The summertime great plains low level jet and the effect of its origin on moisture transport. *Bound-Lay Meteorol*, **88,** 445-466.

Xie, P., M. Chen, and W. Shi, 2010: CPC unified gauge-based analysis of global daily precipitation. *Preprints, 24th Conf. on Hydrology, Atlanta, GA, Amer. Meteor. Soc*.

Xie, P., M. Chen, S. Yang, A. Yatagai, T. Hayasaka, Y. Fukushima, and C. Liu, 2007: A gauge-based analysis of daily precipitation over East Asia. *J Hydrometeorol*, **8,** 607-626.